Combining modelling and experimental approaches to explain how calcium signatures are decoded by CAMTA to produce specific gene expression responses

Junli Liu[1*], Helen J. Whalley[2] & Marc R. Knight[1*]

1. School of Biological and Biomedical Sciences, Durham Centre for Crop Improvement Technology, Durham University, South Road, Durham DH1 3LE, UK

2. Cell Signalling Group, Cancer Research UK Manchester Institute, The University of Manchester, Manchester M20 4BX, UK.

*Joint corresponding authors

Junli Liu: Junli.Liu@durham.ac.uk

Helen Whalley: Helen.Whalley@cruk.manchester.ac.uk

Marc R. Knight: M.R.Knight@durham.ac.uk

Author for correspondence:

Junli Liu (Junli.liu@durham.ac.uk, tel. +44 191 3341376)

Marc R. Knight (M.R.Knight@durham.ac.uk, tel. +44 191 334 1224)

Total word count (excluding summary, references and legends):	**6756**	No. of figures:	**8**
Summary:	**192**	No. of Tables:	**2**
Introduction:	**329**	No of Supporting Information files:	**1**
Materials and Methods:	**1521**		
Results:	**3342**		
Discussion:	**1564**		
Acknowledgements:	**23**		

Summary

- Experimental data show that *Arabidopsis thaliana* is able to decode different calcium signatures to produce specific gene expression responses. It is also known that CAMTA (calmodulin-binding transcription activators) have calmodulin binding domains. Therefore the gene expression responses regulated by CAMTA respond to calcium signals. However, little is known about how different calcium signatures are decoded by CAMTA to produce specific gene expression responses.
- A dynamic model of Ca^{2+}-CaM-CAMTA binding and gene expression responses is developed following thermodynamic and kinetic principles. The model is parameterised using experimental data. Then it is used to analyse how different calcium signatures are decoded by CAMTA to produce specific gene expression responses.
- Modelling analysis reveals 1) calcium signals in the form of cytosolic calcium concentration elevations are nonlinearly amplified by binding of Ca^{2+}, CaM and CAMTA; 2) Amplification of Ca^{2+} signals enables calcium signatures be decoded to give specific CAMTA-regulated gene expression responses; 3) Gene expression responses to a calcium signature depends upon its history and accumulate all the information during the lifetime of the calcium signature.
- Information flow from calcium signatures to CAMTA-regulated gene expression responses has been established by combining experimental data with mathematical modelling.

Keywords: Arabidopsis, calcium signatures, calmodulin, CAMTA, gene expression, mathematical modelling.

Introduction

Plants are sessile organisms and therefore they must adapt their metabolism, growth and architecture to a changing environment. The majority of their defence against stress is realised by changes in gene expression in order to produce proteins required to combat the conditions they encounter. It is thus vital that the correct proteins are produced in response to different environmental conditions i.e. different genes need to be switched on in response to different stimuli. Calcium is a ubiquitous second messenger in eukaryotes and it is a ubiquitous intermediate between stimulus perception and responses in plants. It has been observed that different stimuli produce calcium signatures with different characteristics in plants (McAinsh *et al.*, 1995; Allen *et al.*, 2001; Love *et al.*, 2004; Miwa *et al.*, 2006; McAinsh and Pittman, 2009; Dodd *et al.*, 2010; Kudla et al., 2010; Short *et al.*, 2012). Given that calcium is an intermediate between stimulus-perception and gene expression (Whalley *et al.*, 2011), it is possible that the specific characteristics of the calcium signatures produced by different stresses encode stimulus-specific information. Recent experimental data demonstrate that Arabidopsis is able to decode specific calcium signatures and interpret them, leading to distinct gene expression profiles (Whalley *et al.*, 2011; Whalley and Knight, 2013).

CAMTA are well characterised Ca^{2+}/calmodulin (CaM) -regulated transcription factors (Kim *et al.*, 2009; Galon *et al.*, 2010; Reddy *et al.*, 2011; Bickerton and Pittman, 2012; Poovaiah *et al.*, 2013), and they have CaM-binding domains (Finkler et al. 2007). Therefore, gene expression responses regulated by CAMTA respond to calcium signals (Whalley *et al.*, 2011; Whalley and Knight, 2013).

Although experimental data (Whalley *et al.*, 2011; Whalley and Knight, 2013) show that Arabidopsis is able to decode different calcium signatures to produce specific gene expression responses, little is known about how complex calcium signatures are decoded to generate gene expression responses. In this work, we establish the principles of information flow from calcium signatures to CAMTA-regulated gene expression responses by combining experimental data with mathematical modelling.

Materials and Methods

A dynamic model describing the information flow from calcium signatures to CAMTA-regulated gene expression

The information flow from calcium signatures to CAMTA-regulated gene expression in Arabidopsis is described in Figure 1. The left pane of Figure 1 describes the binding of Ca^{2+}, CaM and CAMTA. CaM has two pairs of Ca^{2+}-binding EF-hand domains located at the N- and C-terminus, respectively (Finn and Forsen, 1995; Valeyev *et al.*, 2008). Ca^{2+} binding kinetics for the pairs of EF-hands at the N and C terminus are significantly different and it displays cooperativity (Linse *et al.*, 1991). The cooperative binding between Ca^{2+} and the four binding sites of CaM has been previously subjected to both experimental and modelling studies (Fajmut *et al.*, 2005; Shifman *et al.*, 2006; Pepke *et al.*, 2010) and the kinetic parameters have been determined (Shifman *et al.*, 2006; Pepke *et al.*, 2010). Table 1 summarises those parameters (Shifman *et al.*, 2006; Pepke *et al.*, 2010). In addition, experimental data show that the CAMTA proteins consist of multiple functional domains associated with binding of CaM and CaM-like proteins (Bouche *et al.*, 2002; Finkler *et al.*, 2007). Mapping of a Ca^{2+} dependent CaM-binding domain in Arabidopsis AtCAMTA1 revealed a single high-affinity binding site (K_d= 1.2e-3 μM) (Bouche *et al.*, 2002; Finkler *et al.*, 2007) and a similar binding site exists in rice (Choi *et al.*, 2005). As binding of Ca^{2+}-CaM complex to CAMTA is tighter than binding of free CaM to CAMTA (Bouche *et al.*, 2002; Finkler *et al.*, 2007), the K_d for R15 in Figure 1 is always larger than 1.2e-3 μM. These parameters are also included in Table 1.

---Figure 1 and Table 1 here---

The unknown equilibrium constants and on/off rates in the left pane of Figure 1 are derived using the detailed balance condition following thermodynamic principles. For example, following the detailed balance condition, equation 1 is always valid.

$$K_{d(R15)}K_{d(R23)} = K_{d(R3)}K_{d(R14)} \qquad \text{(equation 1)}$$

Equation 1 leads to equation 2.

$$K_{d(R23)} = \frac{K_{d(R3)}K_{d(R14)}}{K_{d(R15)}} = K_{d(R3)}P \qquad \text{(equation 2)}$$

As binding of Ca^{2+}-CaM complex to CAMTA is tighter than binding of free CaM to CAMTA (Bouche *et al.*, 2002; Finkler *et al.*, 2007), P is always less than 1 (Table 1). P describes the cooperative binding between CaM and CAMTA in the presence of Ca^{2+}. As P has not been experimentally determined, it is an adjustable parameter in this work. Moreover, as K_d is

K_{off}/K_{on}, the difference between $K_{d(R3)}$ and $K_{d(R23)}$ or the difference between $K_{d(R14)}$ and $K_{d(R15)}$ could be caused by the difference in k_{on}, k_{off} or both. In order to examine the effects of changes in k_{on}, k_{off} or both on modelling results, we define

$$k_{on(R15)} = k_{on(R14)}/Q. \qquad \text{(equation 3)}$$

where Q is an adjustable parameter. If Q=1.0, this implies that cooperativity is realised solely by the changes in k_{off}. Similarly, Q=1/P implies that cooperativity is realised solely by the changes in k_{on}. Other values of Q imply that cooperativity is realised by the changes in both k_{on} and k_{off}. After applying the detailed balance condition following thermodynamic principles to all other loops in Figure 1, the equilibrium constants (K_d) are linked.

Based on experimental data, binding of the Ca^{2+}-CaM complex to CAMTA is tighter than binding of free CaM to CAMTA (Bouche *et al.*, 2002; Finkler *et al.*, 2007). However, experimental measurements are not able to identify the binding affinity of each different Ca^{2+}-CaM complex (i.e. with different numbers of calcium ions at different positions) to CAMTA. Here we assume that the affinity for the binding of any Ca^{2+}-CaM complex to CAMTA is always the same, regardless how many Ca^{2+} binds with CaM. The advantage of this assumption is to greatly reduce adjustable parameters. However, for the sake of completion, we have randomly tested the effects of different binding affinities for the binding between some Ca^{2+}-CaM complexes and CAMTA. Under the conditions that binding of Ca^{2+}-CaM complex to CAMTA is tighter than binding of free CaM to CAMTA (Bouche *et al.*, 2002; Finkler *et al.*, 2007), we have tested the effects of the changes of binding affinity up to two orders with reference to value of 1.2e-3 μM for some Ca^{2+}-CaM complexes (e.g. R20, R33). The qualitative conclusions we will draw in this work do not change if these binding affinities change, as shown in Figures S1, S2, S3, S4. After introducing the detailed balance condition following thermodynamic principles and based on the assumption that the affinity for the binding of any Ca^{2+}-CaM complex to CAMTA is always the same, we are able to derive all other unknown equilibrium constants and on/off rates, as summarised in Table 1.

After using the parameters determined experimentally and introducing thermodynamic constraints, there are only five adjustable parameters left for the left pane of Figure 1, as summarised below. P describes the cooperative binding between CaM and CAMTA in the presence of Ca^{2+}; $k_{on(R14)}$ is the on rate for the binding of Ca^{2+}-CaM complex to CAMTA; Q describes how the cooperative binding between CaM and CAMTA in the presence of $Ca^{2+}$is realised by k_{on}, k_{off} or both. CaM_t describes the total concentration of CaM, which is the

summation of free CaM and all CaM complexes. X_t describes the total concentration of CAMTA, which is the summation of free CAMTA and all CAMTA complexes.

The mass balance of each complex in the left pane of Figure 1 is described using a differential equation, Notes S1. By coupling these differential equations together, we are able to calculate the concentration of any complex for any calcium signature at any time. It is known that $4Ca^{2+}$- CaM is the active CaM -Ca^{2+} binding complex (Pifl *et al.*, 1984). Therefore, this work assumes that the complex $4Ca^{2+}$-CaM-CAMTA (MNNCCX in Figure 1) is the active complex for gene expression response.

The right pane of Figure 1 describes CAMTA-regulated gene expression. CAMTA can be either activators or suppressors of gene expression, as evidenced by the experiments using CAMTA mutants (Galon *et al.*, 2008; Doherty *et al.*, 2009). In addition, the process of gene expression may have multiple entry points of Ca^{2+} signal due to the interactions between Ca^{2+} signal and CAMTA (Miller *et al.*, 2013; Zhang *et al.*, 2014). Clearly, different genes may be regulated by different expression mechanisms. Even if they are regulated by the same mechanism, the parameter values controlling their expression may be different. Moreover, for most genes, gene expression mechanisms have not been experimentally determined. In this work, our focus is to investigate how different calcium signatures are decoded by CAMTA to produce specific gene expression responses. Our primary interest is to establish the information flow from calcium signatures to gene expression rather than the gene expression mechanisms themselves. Therefore, here we use as simple as possible generic gene expression mechanisms. Our method can be generally extended to include any gene expression mechanism by replacing the right pane of Figure 1, if the specific expression mechanism of that specific gene is known.

The simplest gene expression process includes 1) gene transcription is activated or supressed by a transcription factor; and 2) the mRNA is decayed or consumed. The right pane of Figure 1 describes these simplest mechanisms. For category A genes in Figure 1, the differential equation for describing gene expression is as follows.

$$\frac{d[mRNA]}{at} = k_1 + \frac{k_2\left(\frac{[MNNCCX]}{k_4}\right)^n}{1+\left(\frac{[MNNCCX]}{k_4}\right)^n} - k_3[mRNA] \qquad \text{(equation 4)}$$

Where k_1 is the base rate for gene transcription, k_2 is the maximal rate for CAMTA-regulated gene transcription, k_3 is the decay rate constant for the mRNA, k_4 is the binding affinity between $4Ca^{2+}$-CaM-CAMTA complex and DNA, n is Hill coefficient.

Similarly, for category B genes in Figure 1, the differential equation for describing gene expression is as follows.

$$\frac{d[mRNA]}{at} = k_1 + \frac{k_2}{1+\left(\frac{[MNNCCX]}{k_4}\right)^n} - k_3[mRNA] \qquad \text{(equation 5)}$$

The parameters for gene transcription are included in Table 1. In the **Results** section, we will also test and discuss how the parameters relating to gene transcription affects the information flow from calcium signatures to gene expression.

Time Delay

It is evident that the information flow from calcium signatures to changes in gene expression will generally be subjected to a time delay. When a calcium signal emerges, a change in gene expression cannot occur instantly, as the transcriptional pre-initiation complex (containing specific transcription factors e,g, CAMTAs, general transcription factors, mediator and RNA polymerase) needs to be recruited and assembled and an elongation complex needs to form to allows transcription of the coding region (Lee and Young, 2000). In this work, we consider there is a time delay, τ , between calcium signal and gene expression response. After all the concentrations in the left pane of Figure 1 are calculated, the complex $4Ca^{2+}$-CaM-CAMTA induces gene expression after a time delay (τ). The effects of τ on modelling results will be examined.

Numerical Method

The model is implemented using simulator Berkeley Madonna (www.berkeleymadonna.com). Rosenbrock (Stiff) method is used with a tolerance of 1.0e-5. Much smaller tolerances are also tested and the numerical results show that further reduction of tolerances does not improve the accuracy of numerical results. Before a calcium signature is introduced, the system of ordinary differential equations is settled at a steady state using the average Ca^{2+} concentration of the control experiment as an input. When a calcium

signature is introduced, the response of the system of ordinary differential equations is calculated using the time-dependent Ca^{2+} concentration as an input.

Results

Ca^{2+} signals are nonlinearly amplified due to Ca^{2+} - CaM -CAMTA interaction

As shown in Figure 1, under thermodynamic constraints, CaM binds with Ca^{2+}, forming complexes with different numbers of calcium ions at different positions. It is known that $4Ca^{2+}$- CaM is the active CaM -Ca^{2+} binding complex (Pifl et al. 1984). Figures 2, 3 and 4 summarise the amplification of Ca^{2+} signals for three different Ca^{2+} signatures, which were experimentally generated (Whalley et al. 2011). Due to the interaction of Ca^{2+}-CaM-CAMTA, Ca^{2+} signals are nonlinearly amplified into the signals of the active functioning complex $4Ca^{2+}$-CaM-CAMTA.

---Figures 2,3,4 here---

The three Ca^{2+} signatures (Figures 2a, 3a, and 4a) are the inputs for the interaction of Ca^{2+}-CaM-CAMTA (Figure 1), and the respective concentration of the active functioning complex $4Ca^{2+}$-CaM-CAMTA for the three Ca^{2+} signatures are shown in Figures 2b, 3b, and 4b. Figures 2c shows that, for the oscillatory Ca^{2+} signature (Figure 2a), ca. 7 fold change of Ca^{2+} concentration (relative to the experimental measurement of average Ca^{2+} concentration in control experiments) is amplified to ca. 1400 fold change of concentration of $4Ca^{2+}$-CaM-CAMTA complex (relative to the average computed concentration using Ca^{2+} concentration in control experiments). Figure 3c shows that, for the transient Ca^{2+} signature (Figure 3a), ca. 12 fold change of Ca^{2+} concentration is amplified to ca. 8000 fold change of concentration of $4Ca^{2+}$-CaM-CAMTA complex. Similarly, Figure 4c shows that, for the prolonged Ca^{2+} signature (Figure 4a), ca. 3.2 fold change of Ca^{2+} concentration is amplified to ca. 80 fold change of concentration of $4Ca^{2+}$-CaM-CAMTA complex.

Combination of Figures 2 , 3 and 4 reveals that the amplification of Ca^{2+} signals by the interaction of Ca^{2+}-CaM-CAMTA is nonlinear. For example, with reference to the steady-state value of Ca^{2+} concentration and its corresponding concentration of $4Ca^{2+}$-CaM-CAMTA complex, ca. 2-, 4- or 10- fold increase in Ca^{2+} concentrations lead to ca. 10-, 200- or 5000-

fold increase in $4Ca^{2+}$-CaM–CAMTA, respectively. Therefore, although the fold changes of Ca^{2+} concentration in three Ca^{2+} signatures are relatively small, the resulting fold changes of the active complex ($4Ca^{2+}$-CaM–CAMTA) are large and different for each individual signature.

We have further examined how the five adjustable parameters relating to the left pane of Figure 1 affect the modelling results shown in Figures 2-4. The nonlinear fold-change relationship between Ca^{2+} signals and the corresponding active complex ($4Ca^{2+}$-CaM–CAMTA) always exists across a wide range values for these five adjustable parameters, as shown in Figures 5, S5 and S6.

---Figure 5 here---

Figure 5a shows the effects of varying the on rate for the binding between Ca^{2+}-CaM complex and CAMTA ($k_{on(R14)}$) on the amplification of Ca^{2+} signals. For a 4-order change in $k_{on(R14)}$, the amplification of Ca^{2+} signals is qualitatively similar. If $k_{on(R14)}$ is further increased from 100 $\mu M^{-1}s^{-1}$, the amplification of Ca^{2+} signals is similar to the solid line in Figure 5a. However, if $k_{on(R14)}$ is further decreased from 0.01 $\mu M^{-1}s^{-1}$, the amplification of Ca^{2+} signals will be markedly smaller. Figure 5b shows that effects of varying the cooperative binding between CaM and CAMTA in the presence of Ca^{2+} due to on binding rate (Q in equation 3). For a 4-order change, the qualitative trend for the amplification of Ca^{2+} signals is always similar. In addition, we have tested the effects of varying the cooperative binding between CaM and CAMTA in the presence of Ca^{2+} (P in equation 2) in a 3-order range, as P can only be increased to 1.0. Figure S5 shows that the qualitative trend for the amplification of Ca^{2+} signals is always similar. Figure 5c shows that the effects of varying the total CAMTA concentration on the amplification of Ca^{2+} signals. Change of the total CAMTA concentration in a 4-order range gives rise to qualitatively similar amplification of Ca^{2+} signals. In a similar manner, Figure S6 shows that the qualitative trend for the amplification of Ca^{2+} signals is always similar for a 4-order change of the total CaM concentration. In addition, we have also examined the effects of simultaneous variations of all five adjustable parameters. When all parameters are varied, there are a large number of possible combinations. In this work, therefore, we are only able to test certain combinations. As

shown in Figures S7 and S8, the qualitative trend for the amplification of Ca^{2+} signatures is similar when all parameters vary.

Therefore, due to the interaction of Ca^{2+} - CaM -CAMTA, Ca^{2+} signals are always nonlinearly amplified (Figures 2c, 3c and 4c). Moreover, for three different calcium signatures (Figures 2a, 3a, and 4a), due to the differences in the amplitude of Ca^{2+} signatures, the maximum amplification fold change of the three calcium signatures is significantly different (Figures 2, 3 and 4).

Amplification of Ca^{2+} signals enables calcium signatures be decoded to give specific CAMTA-regulated gene expression responses

Experimental data for fold change in CAMTA-regulated gene expression level for three calcium signatures (Figure 2a, 3a and 4a) are included in Table 2. We defined CAMTA-regulated genes as the 20 genes which were induced by any calcium signature described in Whalley et al. 2011 which contained the CAMTA-binding motif 5'-ACGCGT-3' within 500bp of their promoters (Whalley et al. 2011). As shown in Table 2, both oscillatory (Figure 2a) and transient (Figure 3a) calcium signatures are able to induce >1.5 fold expression change in CAMTA-regulated genes, whilst the prolonged (Figure 4a) calcium signature cannot induce >1.5 fold change in any CAMTA-regulated gene (Whalley et al. 2011). As the elevated Ca^{2+} increases CAMTA-regulated gene expression for oscillatory (Figure 2a) and transient (Figure 3a) calcium signatures, we consider that, under our experimental conditions (Whalley et al. 2011), Ca^{2+} only activates (but does not decrease) CAMTA-regulated gene expression (Table 2). Thus, we use equation 4 to calculate the effects of different calcium signatures on CAMTA-regulated gene expression.

The capabilities of Ca^{2+}-CaM-CAMTA interaction in nonlinearly amplifying Ca^{2+} signals allow different calcium signatures to be differentially decoded to generate specific gene expression responses. If Ca^{2+} signals were not amplified by Ca^{2+}-CaM-CAMTA interaction, the fold changes in the three calcium signatures (Figures 2a, 3a and 4a) would be small (from ca. 3.5 fold (for prolonged calcium signature, Figure 4a) to ca. 11 fold (for transient calcium signature, Figure 3a). Such differences in Ca^{2+} signals would be on their own too small to be distinguished and to allow different gene expression responses if they were not amplified. Thus, the role of Ca^{2+}-CaM-CAMTA interaction in amplifying Ca^{2+} signals is important for inducing specific gene expression responses. Figure 6 shows how different calcium

signatures are decoded to generate specific gene expression responses by virtue of the Ca^{2+}-CaM-CAMTA interaction.

---Figure 6 and Table 2 here---

As shown in Figure 6a, due to the large fold-amplification of Ca^{2+} signals in oscillatory and transient calcium signatures (Figures 2a and 3a), large fold-changes in gene expression level are induced. Similarly, due to the small fold-amplification of Ca^{2+} signals in prolonged calcium signatures (Figures 4a), only a small fold-change in gene expression level is induced. Thus, at 1h, the fold change of gene expression level is generally larger than 1.5 fold (Figure 6a) for oscillatory and transient calcium signatures (Figures 2a and 3a), whilst it is less than 1.5 fold (Figure 6a) for the prolonged calcium signature (Figure 4a). Figures S9, S10 and S11 show that fold change for all three calcium signatures at specific time (e.g. 1h) depends on the delay time, which is the time when gene expression starts to responds to Ca^{2+} signals. In Figure 6a, we assume that the delay time is always 600s for three calcium signatures. If we assume that the delay time is different for different genes and/or different calcium signatures, the fold change of gene expression for oscillatory and transient calcium signatures at 1h will change (Figures S9 and S10). However, the fold change of gene expression for prolonged calcium signature is always less than 1.5 fold, independently of the delay time (Figure S11). Thus, Figure 6a explains the experimental observations in Table 2 (Whalley et al. 2011), and it shows that calcium signatures are differentially decoded to give specific CAMTA-regulated gene expression responses.

Modelling analysis further reveals that the binding affinity between $4Ca^{2+}$-CaM-CAMTA complex and DNA is an important parameter for inducing gene expression by calcium signatures. To our knowledge, this parameter has not been experimentally determined. When the binding affinity is reduced to 1.1e-3μM from 1.1e-2μM, all three calcium signatures in Figures 2a, 3a and 4a are able to induce different large fold-changes in gene expression (Figure 6b). At 1h, oscillatory (Figure 2a), transient (Figure 3a) and prolonged (Figure 4a) calcium signature induces ca. 43, 12 and 9 fold change in gene expression, respectively. Thus, Figure 6b shows that even a relatively small fold amplification of calcium signals (e.g., prolonged calcium signature (Figure 4a)) is able to induce a relatively large fold induction of gene expression, with oscillatory calcium signature inducing largest fold change in gene expression . In contrast, the largest fold change in gene expression is induced by transient

calcium signature (Figure 3a) in Figure 6a. Comparison of Figure 6a and 6b shows that the binding affinity between $4Ca^{2+}$-CaM-CAMTA complex and DNA can change how CAMTA-regulated gene expression responds to different calcium signatures. In addition, when the binding affinity is decreased to 1.1e-1μM from 1.1e-2μM, all three calcium signatures in Figures 2a, 3a and 4a are unable to induce fold changes larger than 1.05 in gene expression (Figure 6c). Therefore, gene expression induced by different calcium signatures is quantitatively dependent on the binding affinity between $4Ca^{2+}$-CaM-CAMTA complex and DNA.

In addition, the effects of other parameters relating to gene expression were also examined. Increasing or decreasing k_1 (base rate for gene transcription) or k_2 (maximal rate for $4Ca^{2+}$-CaM-CAMTA complex-regulated gene transcription) by 2 fold does not qualitatively change modelling results (Figures S12 and S13). The Hill coefficient (n) taking the value, 1, 2 or 3 also qualitatively leads to similar results (Figure S14). However, the decay constant of mRNA (k_3) is an important parameter that affects the shape of the curve for gene expression (Figure 6). If k_3 is very small, gene expression continues to increases for the computational time we have tested (2 hours). If k_3 is very large, gene expression approaches the original steady state very quickly. Approximately, a 2-fold increase or decrease of k_3 from its reference value (3.75e-4 s^{-1}) generally maintains the shape of the curve for gene expression as shown in Figure 6 (Figure S15).

Gene expression response to a calcium signature depends on its history during its lifetime

Modelling analysis reveals that the gene expression response to a specific calcium signature depends on its history during its lifetime. Figure 7 shows how this occurs for the oscillatory calcium signature (Figure 2a) using the three binding affinities between $4Ca^{2+}$-CaM-CAMTA complex and DNA, which are used in Figure 6.

---Figure 7 here---

The oscillatory calcium signature (Figure 2a) is nonlinearly amplified into a functional signal ($4Ca^{2+}$-CaM-CAMTA complex) (Figure 2c). In order to understand why the calcium signature induces gene expression in the specific ways described for Figure 6, we calculate the potential steady-state gene expression fold change by varying the $4Ca^{2+}$-CaM-CAMTA complex concentration (solid curve, Figure 7) for three binding affinities between $4Ca^{2+}$-

CaM-CAMTA complex and DNA. The steady-state gene expression fold change represents the maximum possible fold change in gene expression if time is sufficiently long so that steady-state gene expression can become established for each $4Ca^{2+}$-CaM-CAMTA complex concentration. However, when a calcium signature emerges, $4Ca^{2+}$- CaM-CAMTA complex concentration is a transient signal corresponding to the calcium signature and it does not establish a steady state (Figure 2c, 3c, and 4c). Thus, actual gene expression follows the potential, but does not reach the potential, as explained below. At point I in Figure 7a, the oscillatory calcium signature has not emerged yet, and gene expression is at a steady state. When Ca^{2+} concentration elevates (Figure 2a), $4Ca^{2+}$-CaM-CAMTA complex concentration increases. At point II, gene expression has a potential of ca. 800 fold increase. However, $4Ca^{2+}$-CaM-CAMTA complex concentration does not stay at point II and it starts to decrease from point II due to the decrease of Ca^{2+} concentration. At point III, gene expression has a potential of ca. only 10 fold increase. From point III to IV, $4Ca^{2+}$-CaM-CAMTA complex concentration continues to decrease following the calcium signature (Figures 2a-2c), and the potential fold increase of gene expression diminishes. At point IV, gene expression has no potential to increase at all, as $4Ca^{2+}$-CaM-CAMTA complex concentration at point IV is the same as the original steady-state concentration. From point I to IV, gene expression continuously accumulates all the information from the calcium signature. During the first cycle of calcium signature, gene expression increases to 1.6 fold (Figure 7a), although at point II it has the potential of ca. 800-fold increase and at point IV it has the potential to recover to the original steady-state gene expression level, which is the level for which calcium signature has not emerged. At point IV, gene expression memorises the 1.6 fold gene-expression level and uses it as a starting point to read out the second cycle of the calcium signature (Figure 2a). Gene expression response to the second cycle of the calcium signature follows the same principle as that for the first cycle. However, as gene expression memorises the 1.6 fold increase at point IV, at the end of the second cycle, it establishes a ca. 1.9-fold gene expression level (Figure 7a). Again, gene expression response memorises this 1.9-fold increase and continues to read out the third cycle of the calcium signature. After 10 cycles, gene expression increases to ca. 4 fold (point VI). At point VI, the calcium signature (Figure 2a) ends and Ca^{2+} concentration recovers the original steady state level. Correspondingly, $4Ca^{2+}$-CaM-CAMTA complex concentration also recovers its steady state level. Thus, at point VI, gene expression also starts to approach its original steady state level through point VII to point I. From point I to point VII, gene expression has continuously accumulated all the information during the lifetime of this calcium signature. Therefore,

Figure 7a reveals that gene expression response depends on the history of the oscillatory calcium signature (Figure2a) and accumulates all information during the lifetime of this calcium signature

Binding affinity between $4Ca^{2+}$-CaM-CAMTA complex and DNA affects the dependence of gene expression response on the history of a calcium signature. Figures 7b and 7c show that, when the binding affinity is reduced or increased, the curve for the potential fold change of gene expression moves to left or right, respectively. Thus, for the same oscillatory calcium signature (Figure 2a), the reduced or increased binding affinity leads to larger (Figure 7b) or smaller (Figure 7c) gene expression fold changes, respectively. For example, when binding affinity is reduced (Figure 7b), point II corresponds to a ca. 8000-fold potential gene expression change. However, when binding affinity is increased (Figure 7c), point II corresponds to a ca. 2-fold potential gene expression change. This leads to a ca. 16-fold (Figure 7b) and 1.006-fold (Figure 7c) actual gene expression change after the first cycle of the calcium signature, respectively. After 10 cycles of the calcium signature, a ca. 115-fold (Figure 7b) or 1.03-fold (Figure 7c) actual gene expression change has been reached, respectively.

For both the transient calcium signature (Figure 3a) and prolonged calcium signature (Figure 4a), how gene expression depends on the history of a calcium signature can also be analysed using the method summarised in Figure 7. Specifically gene expression accumulates information from both these calcium signatures in a similar manner to the first cycle of Figure 7 (points I to IV), as shown in Figures S16 and S17. Therefore for these two calcium signatures, gene expression also accumulates all information during their lifetimes. In summary, for all three types of calcium signatures (i.e., oscillatory (Figure 2a); transient (Figure3a) and prolonged (Figure 4a) calcium signature), gene expression response always depends on the history of the individual calcium signature and accumulates all information from the individual calcium signature, as shown in Figures 7, S16, S17. This explains phenomena, such as why two signatures with equal areas under the curve (e.g. prolonged and transient) can give different gene expression responses (Whalley *et al.*, 2011).

The three calcium signatures (i.e., oscillatory (Figure 2a); transient (Figure3a) and prolonged (Figure 4a)) examined above have distinctive kinetics. We further investigate how the parameters in oscillations are linked with gene expression. To do so, we reconstruct

piecewise calcium signatures using the oscillatory calcium signature (Figure 2a). For a piecewise calcium signature, the following relationship is always valid.

$$A = \frac{t_{\max}[Ca^{2+}]_{\max} + t_{\min}[Ca^{2+}]_{\min}}{T} \qquad \text{(equation 6)}$$
$$T = t_{\max} + t_{\min}$$

Where A is the average calcium concentration of the calcium signature; t_{max} and t_{min} are the time for calcium concentration to be $[Ca^{2+}]_{max}$ and $[Ca^{2+}]_{min}$, respectively; T is the period. For the oscillatory calcium signature (Figure 2a) A= 0.16μM, T=40s. The average maximum and minimum calcium concentration of the 10 calcium spikes in Figure 2a is $[Ca^{2+}]_{max}$ =0.52 μM and $[Ca^{2+}]_{min}$ =0.10 μM, respectively. Thus, using equation 6, a piecewise calcium signature is constructed (Figure 8a). This piecewise calcium signature has the same key parameters (average, maximum and minimum calcium concentration , period and duration) as those in Figure 2a, but it has a piecewise shape (Figure 8a). Similarly, we can use equation 6 to construct other piecewise calcium signatures with the same key parameters (average, maximum and minimum calcium concentration, duration) as those in Figure 2a, but with different periods (Figures S18 and S19). Due to the difference in oscillatory period, for a duration of 400s, a piecewise oscillatory calcium signature with a period of 8s (Figure S18), 40s (Figure 8a) and 200s (Figure S19) will contain 50, 10 and 2 spikes, respectively. Using the reconstructed three oscillatory calcium signatures, we have investigated how gene expression depends on both the shape and period of calcium signatures (Figure 8b). First, Figure 8b reveals that a piecewise calcium signature induces larger fold change in gene expression than the oscillatory calcium signature in Figure 2a (the curve for the gene expression induced by the reconstructed piecewise calcium signature with a period of 40s in Figure 8b is compared with the curve for the gene expression induced by experimental calcium signature with a period of 40s in Figure 6a). Second, gene expression fold change depends on the period of oscillatory piecewise calcium signatures. Specifically, at 1h, a piecewise oscillatory calcium signature with a period of 8s, 40s and 200s induces 4.8, 6.0 and 6.6 fold change in gene expression, respectively. Thus, for a fixed duration, increasing the number of calcium spikes by decreasing oscillatory period decreases the fold change of gene expression.

---Figure 8 here---

An alternative way to vary the number of calcium spikes is to alter the duration of a calcium signature whilst its oscillatory period is fixed. Figure S20 shows that increasing the number of calcium spikes by increasing the duration of a calcium signature increases the fold change of gene expression. At 1h, a piecewise calcium signature with 5, 40 and 75 spikes induces 1.3, 4.0 and 6.9 fold change in gene expression, respectively. Experimentally, it has been shown that nodulation gene expression is regulated by calcium spike number and the developmental status of the cell (Miwa *et al.*, 2006). Combination of Figures 8b and S20 shows that calcium spike number is an important parameter regulating gene expression in our study. Moreover, both oscillatory period and duration of an oscillatory calcium signature also play their roles in gene expression (Figures 8b and S20). We note that our modelling results (Figures 8b and S20) are only applicable to CAMTA-regulated gene expression and the gene expression mechanism we have used to calculate Figures 8b and S20 is the simple mechanism shown in Figure 1. In general, gene expression may be regulated by other transcription factors and its expression mechanism may be different. In addition, Figure 8b further indicates that the gene expression response represents an accumulation of all information of oscillatory periods in the three piecewise oscillatory calcium signatures during their lifetimes, as the only difference between the three calcium signatures (Figures 8a, S18 and S19) is period.

Discussion

Experimental data show that Arabidopsis is able to decode different calcium signatures to produce specific gene expression responses (Whalley *et al.*, 2011; Whalley and Knight, 2013). Some of these calcium-dependent genes are targets for CAMTA. It is also known that CAMTA have calmodulin binding domains (Finkler *et al.*, 2007). Therefore, gene expression responses regulated by CAMTA respond to calcium signals. In this work, we develop a modelling methodology that establishes the information flow from calcium signatures to CAMTA-regulated gene expression. Specifically, Ca^{2+}-CaM-CAMTA interaction nonlinearly amplifies different calcium signatures. Then, amplification of Ca^{2+} signals allows the calcium signatures to be differentially decoded to give specific CAMTA-regulated gene expression responses. Finally, mathematical modelling reveals that gene expression response depends on the history of a calcium signature and accumulates all information during the lifetime of this calcium signature. This could account for why oscillations of different frequencies can

activate different downstream calcium decoders e.g. CaM kinase II, rather than amplitude and duration of spikes attributed previously (De Koninck and Schulman, 1998).

For plants to survive stress, it is vital that their responses are specific and appropriate to the particular stimulus. This means that the identity of the primary stimulus must be encoded in a "language" the cell can understand. Most stimuli lead to transient elevation in cellular calcium levels. Importantly, different stimuli produce calcium elevations with different characteristics: a unique "calcium signature". Consequently the specific properties of different calcium signatures have been proposed to encode information on the identity of the stimulus (McAinsh *et al.*,1995; Allen *et al.*, 2001; Love *et al.*, 2004; Miwa *et al.*, 2006; McAinsh and Pittman, 2009; Dodd *et al.*, 2010; Short *et al.*, 2012). For example, temperature stress responses are associated with specific calcium signatures (Knight and Knight, 2012). In plants, there are different mechanisms of Ca^{2+}-regulated gene expression (Kim *et al.*, 2009; Galon *et al.*, 2010; Bickerton and Pittman, 2012). One of the possible mechanisms is through the binding of Ca^{2+}, CaM and transcription factors. Using transcription factor CAMTA as an example, this work has developed a general methodology to establish the links between calcium signatures to gene expression. Firstly, Ca^{2+} binds with its target proteins following thermodynamics. This process nonlinearly amplifies Ca^{2+} signal. As the binding of Ca^{2+} with its target proteins may follow different binding mechanisms (Kim *et al.*, 2009; Galon *et al.*, 2010; Bickerton and Pittman, 2012), how different binding processes of Ca^{2+} and its target proteins amplify Ca^{2+} signals should be investigated for each type of transcription factor. As demonstrated in this work, a relatively small fold amplification of signal is able to induce a relatively large fold gene expression (Figure 6b). If the binding affinity between the active complex $4Ca^{2+}$-CaM-CAMTA and DNA is further reduced from that in Figure 6b (1.1e-3 μM), any small fold amplification of signal is able to induce a relatively large fold gene expression. This demonstrates that any, even a modest, calcium signature is able to induce gene expression. This explains how even very modest increases in cytosolic free calcium e.g. in response to ozone can lead to increases in gene expression (Clayton *et al.*, 1999). Moreover, different calcium signatures are thus capable of inducing specific gene expression patterns (Figure 6). Secondly, which Ca^{2+} and protein binding complex is active for DNA binding should be experimentally explored. Based on experimental observation, $4Ca^{2+}$-CaM complex is the active complex for Ca^{2+}-CaM binding (Pifl *et al.*, 1984). Moreover, the binding affinity between active complex and DNA should be measured, as modelling analysis reveals it is a key parameter for specific gene expression responses to calcium signatures.

Thirdly, the mechanisms of gene expression should be investigated for all relevant genes. In particular, Ca^{2+} signals may affect several processes relating to gene expression. For example, it has been proposed that the expression of the downstream genes of EDS1 may be simultaneously positively and negatively regulated by calcium signals (Zhang *et al.*, 2014). In addition, during symbiosis signalling, it has been shown that calcium/calmodulin-dependent protein kinase is negatively and positively regulated by calcium (Miller *et al.*, 2013). For these cases, although the gene expression mechanisms include multiple interaction points with Ca^{2+} signals, how Ca^{2+} signals affect gene expression can also be analysed using the methodology developed in this work. This can be done by introducing more complex gene expression mechanism in the right pane of our Figure 1. In the work presented here, as the gene expression mechanism is generally unknown, we use simplest gene expression mechanisms (Figure 1) to establish the links between calcium signatures and gene expression, demonstrating how different calcium signatures are decoded to produce specific CAMTA-regulated gene expression responses. As actual gene expression mechanisms may be more complicated than what we used in this work, our results shown in Figure 6 can only be qualitatively (not quantitatively) compared with our Table 2. The quantitative fold change of a specific gene should be further investigated if its expression mechanism and the related parameters are determined in the future. Finally, as gene expression response accumulates all information during the lifetime of a calcium signature, it is important to accurately record the kinetics of calcium signatures during its lifetime. This work reveals that the information flow from calcium signatures to gene expression is an integrative dynamical system (Figure 1) following thermodynamic principles. A combined experimental and modelling approach is able to establish this information flow. Based on the experimental data in Table 2, we assume that expression of all genes we have studied in this work is positively regulated by calcium signatures (no downregulated genes were empirically observed). Therefore, we use equation 4 to analyse gene expression. However, if expression of other (non-CAMTA-regulated) genes is negatively regulated by calcium signals, equation 5 should be used to analyse gene expression following the methodology established in this work. The same methodology can also be extended to analyse gene expression regulated by other Ca^{2+}-dependent transcription factors.

Parameterisation of kinetic models is generally a challenging task (Liu *et al.*, 2010; Almquist *et al.*, 2014). In this work, we use the following process to parameterise the kinetic model (Figure 1): 1) using parameters that have been experimentally determined, 2) following

thermodynamic principles to constrain the relationship of parameters, 3) evaluating model sensitivity by varying each of the adjustable parameters, 4) testing model sensitivity for certain parameter combinations by simultaneously varying all adjustable parameters. Our analysis shows that the modelling results presented in this work are robust to variations in the parameter values across a wide range. In addition, whilst our model has integrated a wide range of knowledge about Ca^{2+}-CaM-CAMTA binding, many other aspects relating to Ca^{2+}-CaM-CAMTA binding and activity have not been included in the current model. For instance, different CAMTA isoforms are expressed in different cell types (Mitsuda *et al.*, 2003) and different CAMTA isoforms have been suggested to be involved in responses to different primary signals (Kim *et al.*, 2013; Pandey *et al.*, 2013; Benn *et al.*, 2014). It is also not known whether CAMTA is subject to posttranslational modifications, so this feature is also not included in our model. Therefore, we consider the current model be a starting point for establishing the relationship between calcium signatures and gene expression responses.

Mathematical modelling is an important tool to establish the link between stimulus, calcium signatures and gene expression. Currently, modelling analysis concentrates on different aspects of this link. For example, this work establishes the link from calcium signatures to gene expression for CAMTA-regulated genes in Arabidopsis cells. For other cells such as hepatocytes, various modelling efforts have also been made with an attempt to understand the decoding of calcium signals (Larsen *et al.*, 2004; Schuster *et al.*, 2005; Dupont *et al.*, 2011). Information transfer in Ca^{2+} signalling pathways were also studied by combining experimental data and mathematical modelling (Pahle *et al.*, 2008). In plant cells, other modelling work includes how different calcium signatures are generated from different stimuli. Specifically, a simple model for the cytosolic pool was used to explain the generation of calcium signatures by assuming calcium-permeable channels depend solely on cooling rate and that calcium pumps are dependent on absolute temperature (Plieth 1999). A model of action potential in cells of vascular plants for the cytosolic pool was developed by incorporating K^+, Cl^- and Ca^{2+} channels; H^+ and Ca^{2+} ATPases; $2H^+/Cl^-$ symporter; and H^+/K^+ antiporter. The model supports a hypothesis about participation of H^+ ATPase in AP generation (Vladimir and Vladimir, 2009). Recently, an integrative model that incorporates the interactions of Ca^{2+}, H^+, K^+, Cl^- and ATP in both cytosolic and vacuolar pools reveals how multiple ions in both cytosol and vacuole interplay to shape low temperature calcium signatures in plant cells (Liu *et al.*, 2012). In addition, noisy time series of calcium oscillations (Granqvist *et al.*, 2011) and generation of calcium signatures at other sub-cellular

compartments such as the nucleus (Granqvist *et al.*, 2012) have been studied. All of these and other modelling work in plant cells made efforts to establish links between stimuli and calcium signatures. Thus, it is plausible that, by integrating the links between stimuli and calcium signatures in the literature with the links between calcium signatures and gene expression response as described in this work, future research will be able to establish the relationship of stimuli, calcium signatures and gene expression responses. Thus, an integrative view on calcium signalling in plant cells can be formulated by integrating modelling and experimental study.

Acknowledgements

The authors gratefully acknowledge Research Councils UK and the Biotechnology & Biological Sciences Research Council for funding in support of this study.

References

Allen GJ, Chu SP, Harrington CL, Schumacher K, Hoffmann T, Tang YY, Grill E, Schroeder JI 2001. A defined range of guard cell calcium oscillation parameters encodes stomatal movements. *Nature* 411: 1053-1057.

Almquist J, Cvijovic M, Hatzimanikatis V, Nielsen J, Jirstrand M. 2014. Kinetic models in industrial biotechnology-improving cell factory performance. Metabolic Eng 24: 38–60.

Benn G, Wang CQ, Hicks DR, Stein J, Guthrie C, Dehesh K. 2014. A key general stress response motif is regulated non-uniformly by CAMTA transcription factors. *Plant J* 80: 82-92.

Bouche N, Scharlat A, Snedden W, Bouchez D, Fromm H. 2002. A novel family of calmodulin-binding transcription activators in multicellular organisms. *J. Biol. Chem.* 277: 21851–21861.

Bickerton PD, Pittman JK. 2012. Calcium signalling in plants. In: eLS. John Wiley & Sons, Ltd: Chichester. DOI: 10.1002/9780470015902.a0023722

609 Brown SE, Martin SR, Bayley PM. 1997. Kinetic control of the dissociation pathway of
610 calmodulin-peptide complexes. *J Biol Chem* 272: 3389-3397.

611 Choi MS, Kim MC, Yoo JH, Moon BC, Koo SC, Park BO, Lee JH, Koo YD, Han HJ, Lee
612 SY, Chung WS, Lim CO, Cho MJ. 2005. Isolation of a calmodulin binding transcription
613 factor from rice (Oryza sativa L.). *J. Biol. Chem.* 280: 40820–40831.

614 Clayton H, Knight MR, Knight H, McAinsh MR, Hetherington AM. 1999. Dissection of the
615 ozone-induced calcium signature. *Plant J* 17: 575-579.

616 De Koninck P, Schulman H. 1998. Sensitivity of CaM kinase II to the frequency of Ca2+
617 oscillations. *Science* 279: 227-230.

618 Dodd AN, Kudla J, Sanders D. 2010. The Language of Calcium Signaling. In S. Merchant,
619 W.R. Briggs and D. Ort, eds. *Annual Review of Plant Biology* 61: 593-620.

620 Doherty DJ, Van Buskirk HA, Myers SJ, Thomashow MF. 2009. Roles for Arabidopsis
621 CAMTA transcription factors in cold-regulated gene expression and freezing tolerance. *Plant*
622 *Cell* 21: 972–984.

623 Dupont G, Combettes L, Bird GS, Putney JW. 2011. Calcium oscillations. *Cold Spring*
624 *Harbor Perspectives in Biology* 3: a004226.

625 Fajmut A, Brumen M, Schuster S. 2005. Theoretical model of the interactions between Ca^{2+},
626 calmodulin and myosin light chain kinase. *FEBS Lett* 579: 4361–4366.

627 Finkler A, Ashery-Padan R, Fromm H. 2007. CAMTAs: Calmodulin-binding transcription
628 activators from plants to human. *FEBS Lett.* 581: 3893–98.

629 Finn BE, Forsen S. 1995. The evolving model of calmodulin structure, function and
630 activation. *Structure* 3: 7–11.

631 Gaertner TR, Putkey JA, Waxham MN. 2004. RC3/Neurogranin and Ca^{2+}/calmodulin
632 dependent protein kinase II produce opposing effects on the affinity of calmodulin for
633 calcium. *J Biol Chem* 279: 39374-39382.

634 Galon Y, Finkler A, Fromm H 2010. Calcium-regulated transcription in plants. *Mol. Plant* 3:
635 653–669.

636 Galon Y, Nave R, Boyce JM, Nachmias D, Knight MR, Fromm H. 2008. Calmodulin-
637 binding transcription activator (CAMTA) 3 mediates biotic defense responses in Arabidopsis.
638 *FEBS Lett.* 582: 943–48

639 Granqvist E, Oldroyd GED, Morris RJ. 2011. Automated Bayesian model development for
640 frequency detection in biological time series. *BMC Syst Biol* 5: 97.

641 Granqvist E, Wysham D, Hazledine S, Kozlowski W, Sun J, Charpentier M, Martins TV,
642 Haleux P, Tsaneva-Atanasova K, Downie JA, Oldroyd GED, Morris RJ. 2012. Buffering
643 capacity explains signal variation in symbiotic calcium oscillations. *Plant Physiol* 160: 2300-
644 2310.

645 Kim MC, Chung WS, Yun DJ, Cho MJ. 2009. Calcium and calmodulin-mediated regulation
646 of gene expression in plants. *Mol. Plant* 2: 13-21.

647 Kim Y, Park S, Gilmour SJ, Thomashow MF. 2013. Roles of CAMTA transcription factors
648 and salicylic acid in configuring the low-temperature transcriptome and freezing tolerance of
649 Arabidopsis. *Plant J* 75: 364-376.

650 Knight MR, Knight H. 2012. Low-temperature perception leading to gene expression and
651 cold tolerance in higher plants. *New Phytol* 195: 737-751.

652 Kubota Y, Putkey J, Waxham M. 2007. Neurogranin controls the spatiotemporal pattern of
653 postsynaptic Ca^{2+}/CaM signaling. *Biophys J* 93: 3848-3859.

654 Kudla J, Batistic O, Hashimoto K. 2010. Calcium signals: The lead currency of plant
655 information processing. *Plant Cell* 22: 541–563.

656 Larsen AZ, Olsen LF, Kummer U. 2004. On the encoding and decoding of calcium signals in
657 hepatocytes. *Biophys Chem* 107: 83–99.

658 Lee TI, Young RA. 2000. Transcription of eukaryotic protein-coding genes. *Annu Rev Genet*
659 34: 77-137.

660 Linse S, Helmersson A, Forsen S. 1991. Calcium binding to calmodulin and its globular
661 domains. *J Biol Chem* 266: 8050–8054.

662 Liu JL, Grieson CS, Webb AAR, Hussey PJ. 2010. Modelling dynamic plant cells. *Current*
663 *Opinion in Plant Biology* 13: 744–749.

664 Liu JL, Knight H, Hurst CH, Knight MR. 2012. Modelling and experimental analysis of the
665 role of interacting cytosolic and vacuolar pools in shaping low temperature calcium
666 signatures in plant cells. *Mol Biosyst* 8: 2205-2220.

667 Love J, Dodd AN, Webb AAR. 2004. Circadian and diurnal calcium oscillations encode
668 photoperiodic information in Arabidopsis. *Plant Cell* 16: 956–966.

669 Martin S, Maune J, Beckingham K, Bayley P. 1992. Stopped-flow studies of calcium
670 dissociation from calcium-binding-site mutants of Drosophila melanogaster calmodulin.
671 *European Journal of Biochemistry* 205: 1107-1114.

672 McAinsh MR, Pittman JK. 2009. Shaping the calcium signature. *New Phytol.* 181: 275–294.

673 McAinsh MR, Webb AAR, Taylor JE, Hetherington AM. 1995. Stimulus-induced
674 oscillations in guard cell cytosolic-free calcium. *Plant Cell* 7: 1207–1219.

675 Miller JB, Pratap A, Miyahara A, Zhou L, Bornemann S, Morris RJ, Oldroyd GE. 2013.
676 Calcium/calmodulin-dependent protein kinase is negatively and positively regulated by
677 calcium, providing a mechanism for decoding calcium responses during symbiosis signaling.
678 *Plant Cell* 25: 5053–5066.

679 Mitsuda N, Isono T, Sato MH. 2003. Arabidopsis CAMTA family proteins enhance V-PPase
680 expression in pollen. *Plant Cell Physiol* 44: 975-981.

681 Miwa H, Sun J, Oldroyd GED, Downie JA. 2006. Analysis of calcium spiking using a
682 cameleon calcium sensor reveals that nodulation gene expression is regulated by calcium
683 spike number and the developmental status of the cell. *Plant Journal* 48: 883–894.

684 Pahle J, Green A, Dixon C, Kummer U. 2008. Information transfer in signaling pathways: a
685 study using coupled simulated and experimental data. *BMC Bioinformatics* 9: 139.

686 Pandey N, Ranjan A, Pant P, Tripathi RK, Ateek F, Pandey HP, Patre UV, Sawant SV. 2013.
687 CAMTA 1 regulates drought responses in *Arabidopsis thaliana*. *BMC Genomics* 14: 216.

688 Peersen OB, Madsen TS, Falke JJ. 1997. Intermolecular tuning of calmodulin by target
689 peptides and proteins: differential effects on Ca2+ binding and implications for kinase
690 activation. *Protein Sci* 6: 794-807.

691 Pepke S, Kinzer-Ursem T, Mihalas S, Kennedy MB. 2010. A dynamic model of interactions
692 of Ca^{2+}, calmodulin, and catalytic subunits of Ca^{2+}/calmodulin-dependent protein kinase II.
693 *PLoS Comput Biol* 6: e1000675. doi: 10.1371/journal.pcbi.1000675.

694 Persechini A, White HD, Gansz KJ. 1996. Different mechanisms for Ca^{2+} dissociation from
695 complexes of calmodulin with nitric oxide synthase or myosin light chain kinase. *J Biol*
696 *Chem* 271: 62-67.

697 Pifl C, Plank B, Wyskovsky W, Bertel O, Hellmann G, Suko J. 1984. Calmodulin X $(Ca^{2+})_4$
698 is the active calmodulin-calcium species activating the calcium-, calmodulin-dependent
699 protein kinase of cardiac sarcoplasmic reticulum in the regulation of the calcium pump.
700 *Biochim. Biophys. Acta* 773: 197-206.

701 Plieth C. 1999. Temperature sensing by plants: calcium-permeable channels as primary
702 sensors-A model. *J. Membrane Biol.* 172: 121–127.

703 Poovaiah BW, Du L, Wang H, Yang T. 2013. Recent advances in calcium/calmodulin-
704 mediated signaling with an emphasis on plant-microbe interactions. *Plant Physiol.* 163: 531–
705 542.

706 Reddy ASN, Ali GS, Celesnik H, Day, IS. 2011. Coping with stresses: roles of calcium- and
707 calcium/calmodulin-regulated gene expression. *Plant Cell* 23: 2010–2032.

708 Schuster S, Knoke B, Marhl M. 2005. Differential regulation of proteins by bursting calcium
709 oscillations-a theoretical study. *BioSystems* 81: 49–63.

710 Shifman JM, Choi MH, Mihalas S, Mayo SL, Kennedy MB. 2006. Ca^{2+}/Calmodulin
711 dependent protein kinase II (CaMKII) is activated by calmodulin with two bound calciums.
712 *Proc Natl Acad Sci U S A* 103: 13968-13973.

713 Short EF, North KA, Roberts MR, Hetherington AM, Shirras AD, McAinsh MR. 2012. A
714 stress-specific calcium signature regulating an ozone-responsive gene expression network in
715 Arabidopsis. *Plant Journal* 71: 948–961.

716 Valeyev N, Bates D, Heslop-Harrison P, Postlethwaite I, Kotov N. 2008. Elucidating the
717 mechanisms of cooperative calcium-calmodulin interactions: a structural systems biology
718 approach. *BMC Systems Biology* 2: 48. doi: 10.1186/1752-0509-2-48.

719 Vladimir S, Vladimir V. 2009. A mathematical model of action potential in cells of vascular
720 plants. *J Membrane Biol.* 232: 59–67.

721 Whalley HJ, Knight MR. 2013. Calcium signatures are decoded by plants to give specific
722 gene responses. *New Phytol.* 197: 690–693.

723 Whalley HJ, Sargeant AW, Steele JFC, Lacoere T, Lamb R, Saunders NJ, Knight H, Knight
724 MR. 2011. Transcriptomic analysis reveals calcium regulation of specific promoter motifs in
725 Arabidopsis. *Plant Cell* 23: 4079–4095.

726 Zhang L, Du L, Shen C, Yang Y, Poovaiah BW. 2014. Regulation of plant immunity through
727 ubiquitin-mediated modulation of Ca(2+) -calmodulin-AtSR1/CAMTA3 signaling. *Plant J*
728 78: 269–281.

729

730 **Fig. S1** The effects of varying K_d of R33, $K_{d(R33)}$, by changing kon.

731 **Fig. S2** The effects of varying K_d of R33, $K_{d(R33)}$, by changing koff.

732 **Fig. S3** The effects of varying K_d of R20, $K_{d(R20)}$, by changing kon.

733 **Fig. S4** The effects of varying K_d of R20, $K_{d(R20)}$, by changing koff.

734 **Fig. S5** The effects of varying the cooperative binding between CaM and CAMTA in the
735 presence of Ca^{2+}.

736 **Fig. S6** The effects of varying the total CaM concentration on the amplification of Ca^{2+}
737 signals.

738 **Fig. S7** The effects of simultaneously varying all five adjustable parameters (example 1).

739 **Fig. S8** The effects of simultaneously varying all five adjustable parameters (example 2).

740 **Fig. S9** Dependence of fold change in gene expression induced by oscillatory calcium
741 signature (Figure 2a) on the delay time.

742 **Fig. S10** Dependence of fold change in gene expression induced by transient calcium
743 signature (Figure 3a) on the delay time.

744 **Fig. S11** Dependence of fold change in gene expression induced by prolonged calcium

745 signature (Figure 4a) on the delay time.

746 **Fig. S12** The effects of varying base rate for gene transcription (k_1) on fold change of gene

747 expression.

748 **Fig. S13** The effects of varying maximal rate for $4Ca^{2+}$-CaM-CAMTA complex-regulated

749 gene transcription (k_2) on fold change of gene expression.

750 **Fig. S14** The effects of varying Hill coefficient (n) on fold change of gene expression.

751 **Fig. S15** The effects of varying the decay constant of mRNA (k_3) on fold change of gene

752 expression.

753 **Fig. S16** Gene expression accumulates all information during the lifetime of the transient

754 calcium signature (Figure 3a).

755 **Fig. S17** Gene expression accumulates all information during the lifetime of the prolonged

756 calcium signature (Figure 4a).

757 **Fig. S18** The reconstructed piecewise calcium signature with T=8s.

758 **Fig. S19** The reconstructed piecewise calcium signature with T=200s.

759 **Fig. S20** Effects of the number of calcium spikes on fold change in gene expression.

760 **Notes S1** Modelling equations.

761

762

763

764 Figure legends

765 Figure 1. A dynamic model that describes the information flow from calcium signatures to
766 CAMTA-regulated gene expression in Arabidopsis. Left pane: Ca^{2+}, CaM and CAMTA bind
767 to form different complexes. When [Ca^{2+}] changes, this binding process responds following
768 thermodynamic principles. Right pane: gene expression is regulated by the active complex
769 $4Ca^{2+}$-CaM-CAMTA (M_{NNCCX}) using the two simplest gene expression mechanisms. Figure
770 1 is a generic model for studying the information flow from calcium signatures to CAMTA-
771 regulated gene expression.

772 Figure 2. Oscillatory calcium signature induced in experiments that use controlled electrical
773 stimulations (Whalley *et al.*, 2011) and amplification of Ca^{2+} signal due to Ca^{2+}-CaM-
774 CAMTA binding in Arabidopsis. a). Solid line: experimental Ca^{2+} elevation. Dashed line:
775 control. b). Computational results for response of the active complex $4Ca^{2+}$-CaM-CAMTA to
776 the calcium signature (solid line) and to the control experiment (dashed line), respectively. c).
777 Fold-change analysis shows that Ca^{2+} signals are nonlinearly amplified by Ca^{2+}-CaM-
778 CAMTA binding.

779 Figure 3. Transient calcium signature induced in experiments that use controlled electrical
780 stimulations (Whalley *et al.*, 2011) and amplification of Ca^{2+} signal due to Ca^{2+}-CaM-
781 CAMTA binding in Arabidopsis. a). Solid line: experimental Ca^{2+} elevation. Dashed line:
782 control. b). Computational results for response of the active complex $4Ca^{2+}$-CaM-CAMTA to
783 the calcium signature (solid line) and to the control experiment (dashed line), respectively. c).
784 Fold-change analysis shows that Ca^{2+} signals are nonlinearly amplified by Ca^{2+}-CaM-
785 CAMTA binding.

786 Figure 4. Prolonged calcium signature induced in experiments that use controlled electrical
787 stimulations (Whalley *et al.*, 2011) and amplification of Ca^{2+} signal due to Ca^{2+}-CaM-
788 CAMTA binding in Arabidopsis. a). Solid line: experimental Ca^{2+} elevation. Dashed line:
789 control. b). Computational results for response of the active complex $4Ca^{2+}$-CaM-CAMTA to
790 the calcium signature (solid line) and to the control experiment (dashed line), respectively. c).
791 Fold-change analysis shows that Ca^{2+} signals are nonlinearly amplified by Ca^{2+}-CaM-
792 CAMTA binding.

Figure 5. Evaluating the effects of the adjustable parameters on the amplification of Ca^{2+} signals. a): Effects of altering the on rate for the binding between the Ca^{2+}-CaM complex and CAMTA ($k_{on(R14)}$) on the amplification of Ca^{2+} signals. Solid line: $k_{on(R14)}$=100 $\mu M^{-1}s^{-1}$. Dashed line: $k_{on(R14)}$=0.01 $\mu M^{-1}s^{-1}$. The reference value is $k_{on(R14)}$=1 $\mu M^{-1}s^{-1}$ (Figure 2). b): Effects of altering the cooperative binding between CaM and CAMTA in the presence of Ca^{2+}due to on binding rate (Q in equation 3) on the amplification of Ca^{2+} signals. Solid line: Q=0.01 $\mu M^{-1}s^{-1}$. Dashed line: Q=100 $\mu M^{-1}s^{-1}$. The reference value is Q=1 $\mu M^{-1}s^{-1}$ (Figure 2). c): Effects of altering the total CAMTA concentration on the amplification of Ca^{2+} signals. Solid line: X_t=1000 μM. Dashed line: X_t=0.1 μM. The reference value is 10 μM (Figure 2).

Figure 6. Fold change in gene expression induced by three different calcium signatures with three binding affinities between the active complex $4Ca^{2+}$-CaM-CAMTA and DNA in Arabidopsis. The delay time between calcium signature and gene expression is 600s for all three calcium signatures. a): Binding affinity (K_d) is 1.1e-2 μM. Both oscillatory and transient calcium signatures induce ca. 2-fold gene expression increase at 1h, while prolonged calcium signature induces ca. 1.05-fold gene expression increase at 1h. b): Binding affinity (K_d) is 1.1e-3 μM. Oscillatory, transient and prolonged calcium signatures induce ca. 43-, 12- and 9-fold gene expression increase at 1h, respectively. c) Binding affinity is (K_d) 1.1e-1 μM. Oscillatory, transient and prolonged calcium signatures all induce less than 1.02-fold gene expression increase at 1h.

Figure 7. Gene expression accumulates all information during the lifetime of the oscillatory calcium signature (Figure 2a) for three binding affinities between the active complex $4Ca^{2+}$-CaM-CAMTA and DNA in Arabidopsis. Solid line (Right y-axis): potential fold change of gene expression if the concentration of $4Ca^{2+}$-CaM-CAMTA stays at each concentration sufficiently long enough that a steady-state is established at each concentration. Dashed line (left y-axis): actual fold change of gene expression for 10 cycles of Ca^{2+} oscillation (Figure 2a). Binding affinity (K_d) between the active complex $4Ca^{2+}$ - CaM -CAMTA and DNA: a) 1.1e-2 μM. b) 1.1e-3 μM. c) 1.1e-1 μM.

Figure 8. Fold change in gene expression induced by three piecewise calcium signatures that are reconstructed using the oscillatory calcium signature (Figure 2a). Binding affinity (K_d) between the active complex $4Ca^{2+}$ - CaM -CAMTA and DNAis 1.1e-2 μM. a) the reconstructed piecewise calcium signature with A= 0.16μM, $[Ca^{2+}]_{max}$ =0.52 μM and

825 $[Ca^{2+}]_{min}$ =0.10 μM, T=40s. b) Fold change in gene expression induced by three piecewise

826 calcium signatures: bottom: T=8s (Figure S18); middle: T=40s (Figure 8a);

827 Top: T=200s (Figure S19).

828

829 Table 1. Parameters for the model described in Figure 1.

1. Parameters derived using experimental data for the binding of Ca^{2+}, CaM and CAMTA (Left pane of Figure 1)			
Reaction	Reaction description	Equilibrium constant (K_d)	Kinetic constants (k_{on}; k_{off})
R1, R9, R11	binding of first Ca^{2+} to CaM C-terminus	10μM (Linse *et al.* (1991); Shifman *et al.* (2006); Kubota *et al.* (2007); Pepke *et al.* (2010))	k_{on}=4 $\mu M^{-1}s^{-1}$; k_{off}=40 s^{-1}. (Martin *et al.* (1992); Persechini *et al.* (1996); Gaertner *et al.* (2004); Pepke *et al.* (2010))
R2, R10, R12	binding of second Ca^{2+} to CaM C-terminus	0.925μM (Linse *et al.* (1991); Shifman *et al.* (2006); Kubota *et al.* (2007); Pepke *et al.* (2010))	k_{on}=10 $\mu M^{-1}s^{-1}$; k_{off}=9.25 s^{-1}. (Gaertner *et al.* (2004); Pepke *et al.* (2010))
R3,R5,R7	binding of first Ca^{2+} to CaM N-terminus	25μM (Linse *et al.* (1991); Shifman *et al.* (2006); Kubota *et al.* (2007); Pepke *et al.* (2010))	k_{on}=100$\mu M^{-1}s^{-1}$; k_{off}=2500 s^{-1}. (Brown *et al.* (1997); Peersen *et al.* (1997); Gaertner *et al.* (2004); Pepke *et al.* (2010))
R4,R6,R8	binding of second Ca^{2+} to CaM N-terminus	5μM (Linse *et al.* (1991); Shifman *et al.* (2006); Kubota *et al.* (2007); Pepke *et al.* (2010))	k_{on}=150$\mu M^{-1}s^{-1}$; k_{off}=750 s^{-1}. (Brown *et al.* (1997); Peersen *et al.* (1997); Gaertner *et al.* (2004); Pepke *et al.* (2010))
R14	binding of Ca^{2+}-CaM complex to CAMTA	1.2e-3μM (Bouche *et al.* (2002); Finkler *et al.* (2007))	k_{on}=1$\mu M^{-1}s^{-1}$; k_{off}=1.2e-3 s^{-1} Notes: k_{on} is an adjustable parameter in this work. $k_{off}=K_d k_{on}$
R15	binding of free CaM to CAMTA	$K_{d(R14)}/P$=1.2e-3μM/P. P=0.1 , which is always smaller than 1, is an adjustable parameter, indicating that binding of Ca^{2+}-CaM complex to CAMTA is tighter than binding of free CaM to CAMTA (Bouche *et al.* (2002); Finkler *et al.* (2007))	$k_{on} = k_{on(R14)}/Q$. Q=1.0 is an adjustable parameter and it describes the cooperative binding between CaM and CAMTA in the presence of Ca^{2+}due to on binding rate. $k_{off}=K_d k_{on}= (K_{d(R14)} k_{on(R14)})/(PQ)= k_{off(R14)} /(PQ)$.
2. Parameters derived based on the detailed balance conditions following thermodynamic principle and the assumption that the affinity for the binding of any Ca^{2+}-CaM complex to CAMTA is always the same (Left pane of Figure 1)			
$K_{d(R13)}=K_{d(R14)}=k_{d(R16)}=k_{d(R17)}=K_{d(R18)}=K_{d(R19)}=K_{d(R20)}=K_{d(R33)}$, $K_{d(R2)}=K_{d(R22)}$, $K_{d(R4)}=K_{d(R24)}$, $K_{d(R5)}=K_{d(R25)}$, $K_{d(R6)}=K_{d(R26)}$, $K_{d(R7)}=K_{d(R27)}$, $K_{d(R8)}=K_{d(R28)}$, $K_{d(R9)}=K_{d(R29)}$, $K_{d(R10)}=K_{d(R30)}$, $K_{d(R11)}=K_{d(R31)}$, $K_{d(R12)}=K_{d(R32)}$. As long as the binding affinities (K_d) for two reactions are the same, we consider their respective k_{on} and k_{off} are also the same.			
3. Parameters for gene expression (right pane of Figure 1)			
$k_1 = 5.0\times10^{-6}$ μM s^{-1}, $k_2 = 5.0\times10^{-2}$ μM s^{-1}, $n = 2$, $k_3 = 3.75\times10^{-4}$ s^{-1}, $k_4 = 1.1\times10^{-2}$ μM			

830

831 Table 2. Experimental results for the fold change of CAMTA-regulated gene expression at 1h
832 in Arabidopsis for the three calcium signatures that were induced using controlled electrical
833 stimulations (Whalley et al. (2011)). "Not induced" is referred to <1.5-fold change (Whalley
834 et al. (2011)).

AGI	**Fold change for oscillatory calcium signature Figure2a**	**Fold change for transient calcium signature Figure3a**	**Fold change for prolonged calcium signature Figure 4a**
AT2G20630	3.13	2.36	Not induced
AT3G10300	Not induced	2.14	Not induced
AT3G18420	1.71	2.06	Not induced
AT1G19180	1.54	2.26	Not induced
AT5G15650	1.80	2.27	Not induced
AT3G05500	3.14	3.90	Not induced
AT1G07890	1.58	2.12	Not induced
AT1G18610	Not induced	4.56	Not induced
AT1G19380	1.89	2.29	Not induced
AT1G63750	3.08	No data	Not induced
AT3G03020	1.82	2.11	Not induced
AT3G19150	2.20	1.85	Not induced
AT3G43680	Not induced	5.49	Not induced
AT3G45970	Not induced	2.02	Not induced
AT4G19200	2.18	2.02	Not induced
AT4G22610	1.62	1.99	Not induced
AT4G29670	2.26	1.89	Not induced
AT4G30210	1.74	2.53	Not induced
AT5G24810	2.11	2.06	Not induced
AT5G45350	2.40	3.24	Not induced

835

836

837

Calcium, CaM and CAMTA bind to form different complexes

Calcium signatures, [Ca^{2+}]

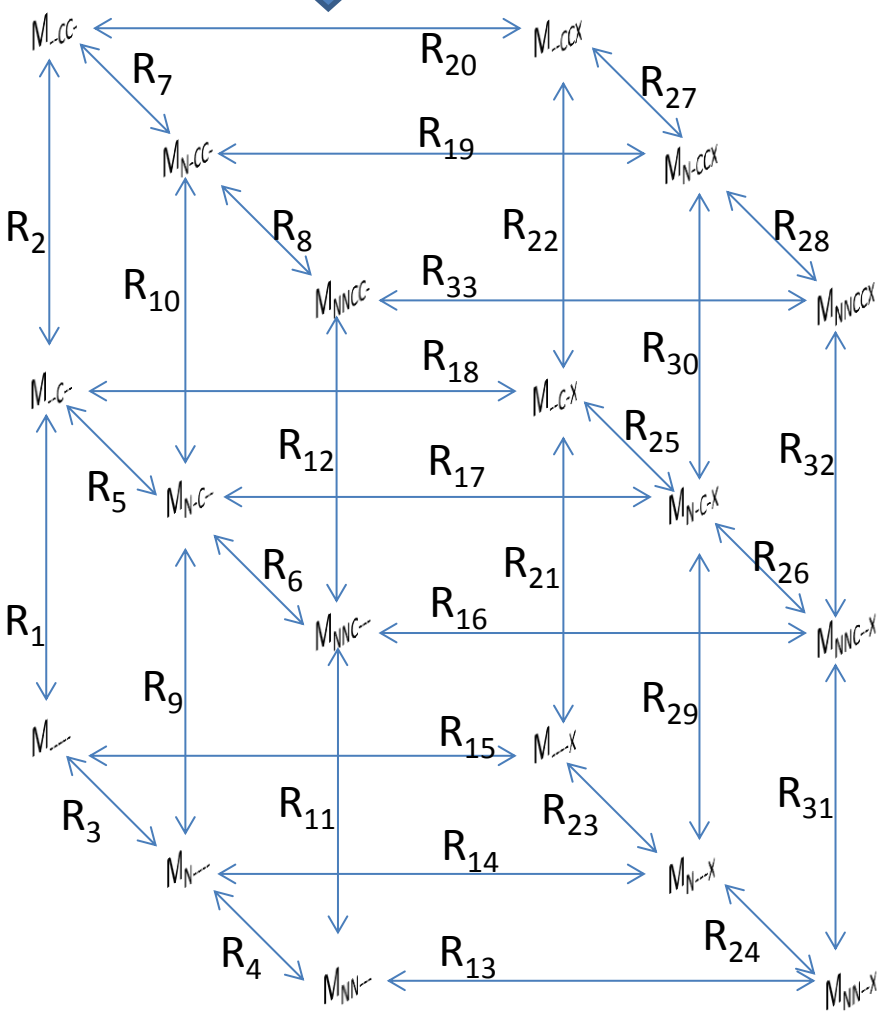

Gene expression

Genes are classified into two categories: Category A is positively regulated by $4Ca^{2+}$–CaM-CAMTA complex. Category B is negatively regulated by $4Ca^{2+}$–CaM-CAMTA complex.

Category A genes

→ mRNA →

Category B genes

→ mRNA →

M: CaM
C: 1 Ca^{2+} binding to C-terminus of CaM
N: 1 Ca^{2+} binding to N-terminus of CaM
X: CAMTA
mRNA: mRNA transcribed from the genes regulated by $4Ca^{2+}$–CaM-CAMTA complex

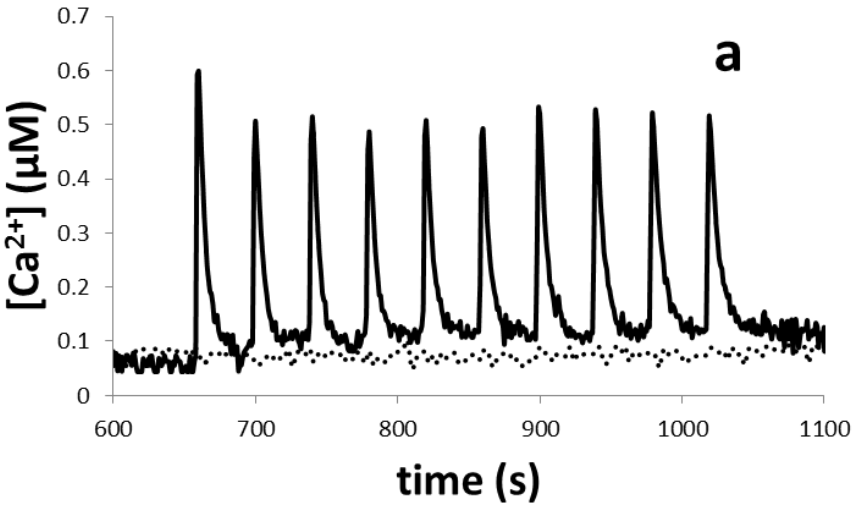
a
[Ca2+] (µM)
0.7
0.6
0.5
0.4
0.3
0.2
0.1
0
600
700
800
900
1000
1100
time (s)

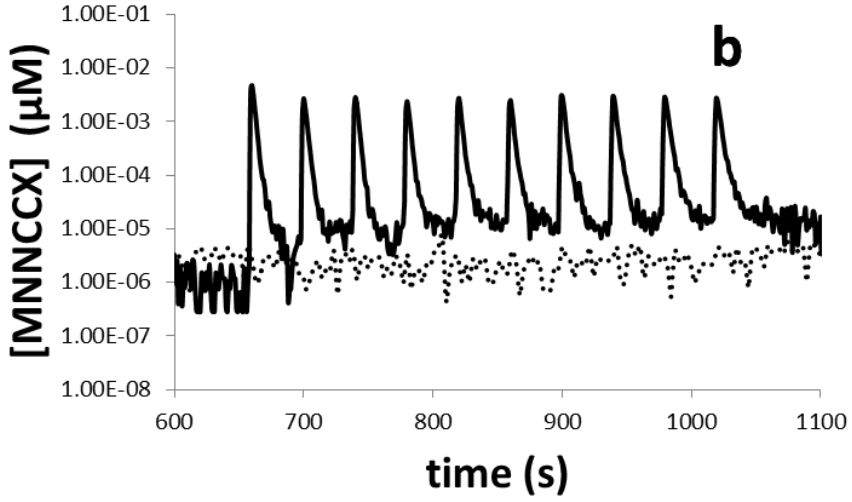
b
[MNNCCX] (µM)
1.00E-01
1.00E-02
1.00E-03
1.00E-04
1.00E-05
1.00E-06
1.00E-07
1.00E-08
600
700
800
900
1000
1100
time (s)

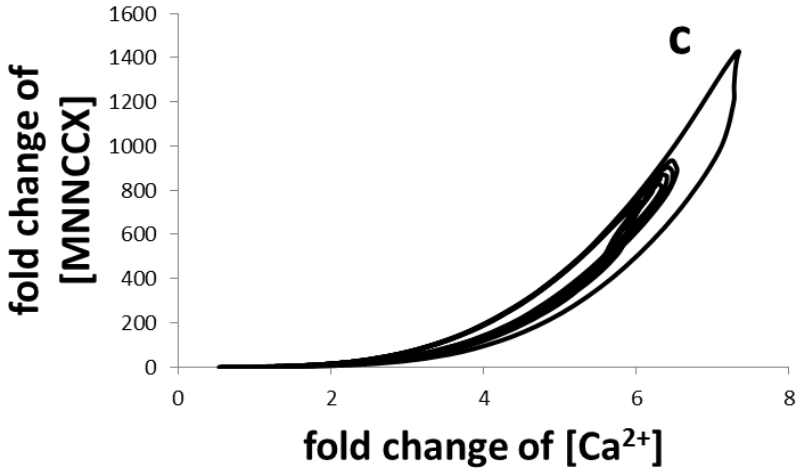
c
fold change of [MNNCCX]
1600
1400
1200
1000
800
600
400
200
0
0
2
4
6
8
fold change of [Ca2+]

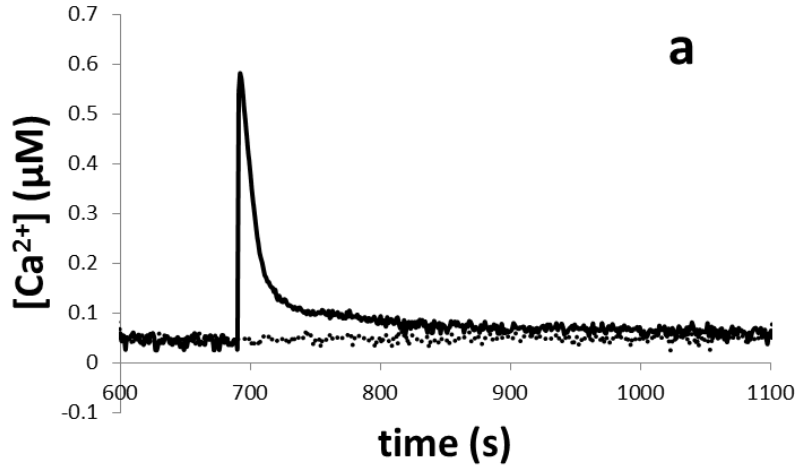
a
[Ca2+] (µM)
0.7
0.6
0.5
0.4
0.3
0.2
0.1
0
-0.1
600
700
800
900
1000
1100
time (s)

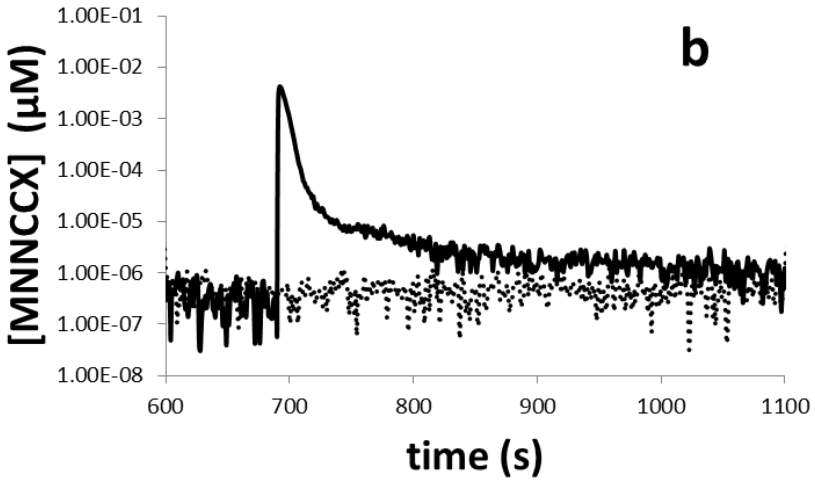
b
[MNNCCX] (µM)
1.00E-01
1.00E-02
1.00E-03
1.00E-04
1.00E-05
1.00E-06
1.00E-07
1.00E-08
600
700
800
900
1000
1100
time (s)

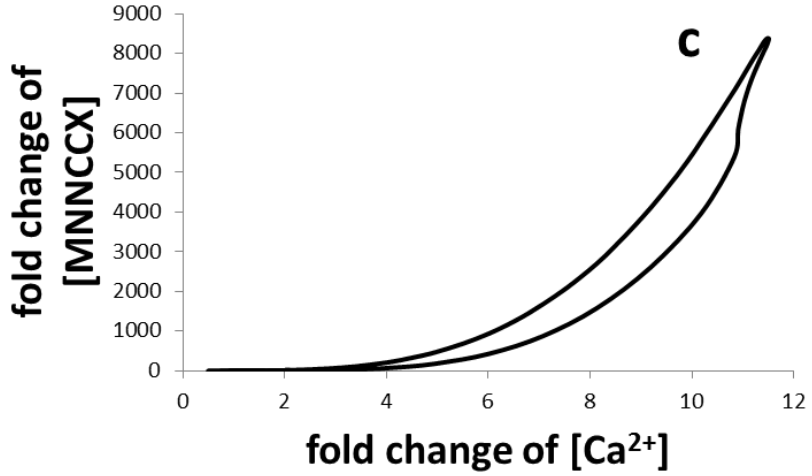
c
fold change of [MNNCCX]
9000
8000
7000
6000
5000
4000
3000
2000
1000
0
0
2
4
6
8
10
12
fold change of [Ca2+]

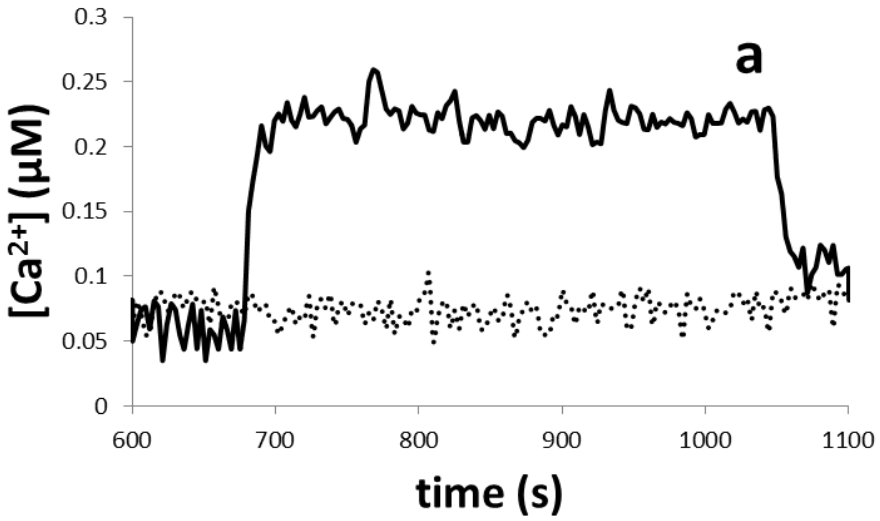
a
0.3
0.25
0.2
0.15
0.1
0.05
0
[Ca2+] (μM)
600
700
800
900
1000
1100
time (s)

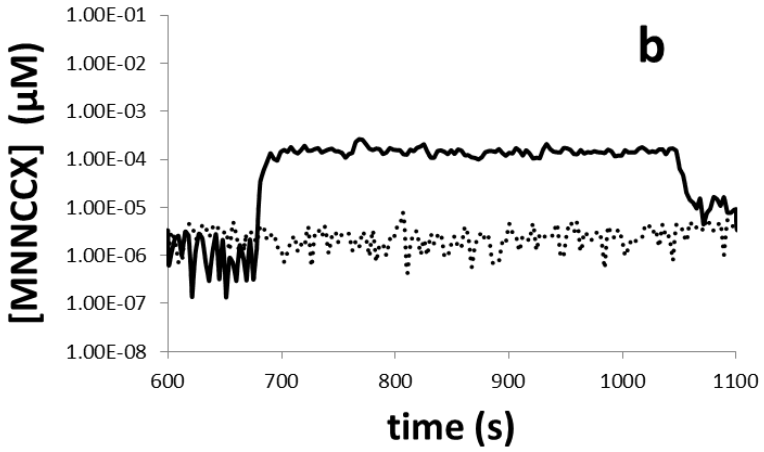
b
1.00E-01
1.00E-02
1.00E-03
1.00E-04
1.00E-05
1.00E-06
1.00E-07
1.00E-08
[MNNCCX] (μM)
600
700
800
900
1000
1100
time (s)

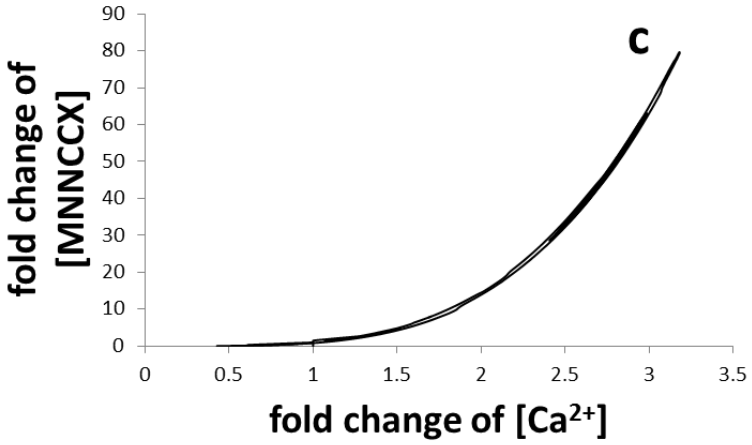
c
90
80
70
60
50
40
30
20
10
0
fold change of [MNNCCX]
0
0.5
1
1.5
2
2.5
3
3.5
fold change of [Ca2+]

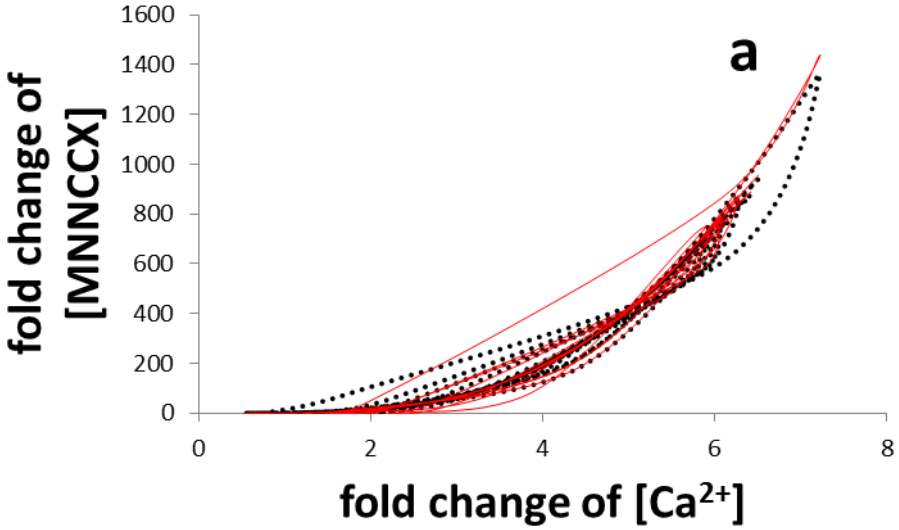
a
fold change of [MNNCCX]
1600
1400
1200
1000
800
600
400
200
0
0
2
4
6
8
fold change of [Ca2+]

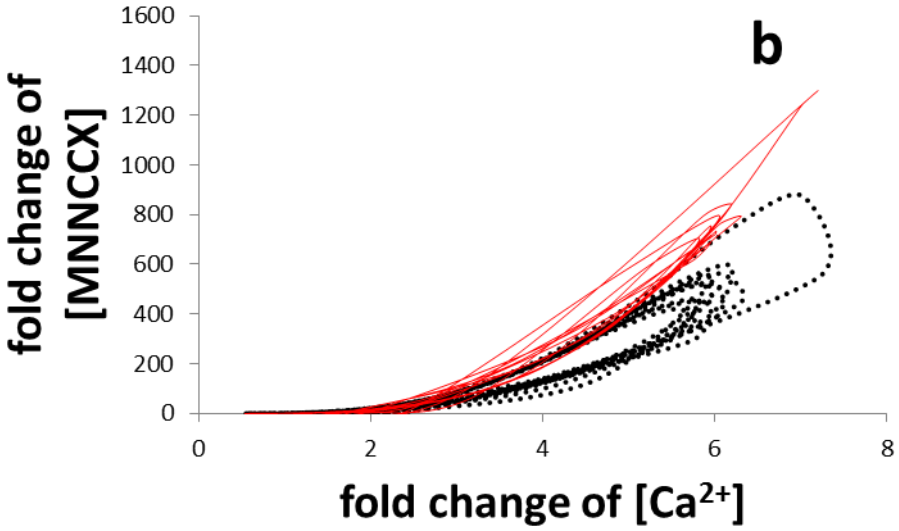
b
fold change of [MNNCCX]
1600
1400
1200
1000
800
600
400
200
0
0
2
4
6
8
fold change of [Ca2+]

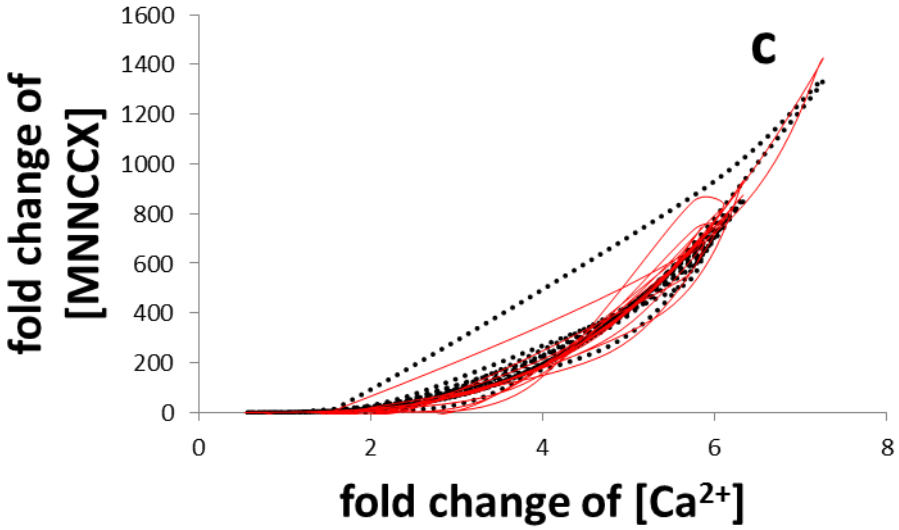
c
fold change of [MNNCCX]
1600
1400
1200
1000
800
600
400
200
0
0
2
4
6
8
fold change of [Ca2+]

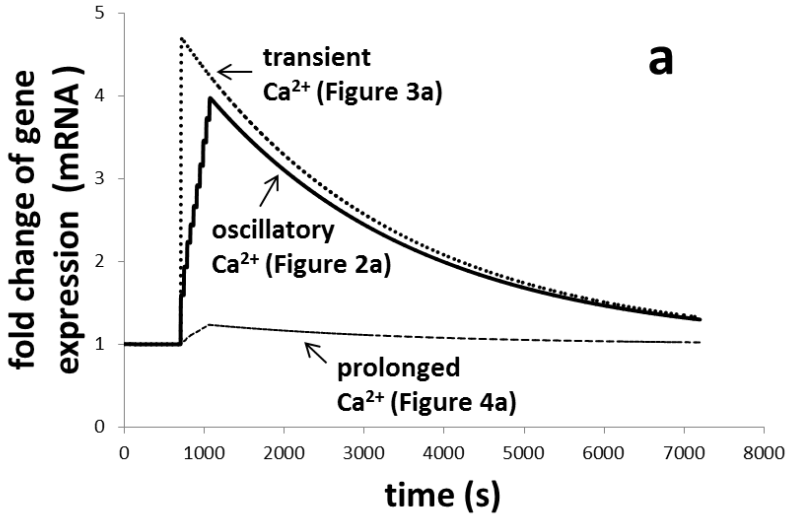
a
transient
Ca2+ (Figure 3a)
oscillatory
Ca2+ (Figure 2a)
prolonged
Ca2+ (Figure 4a)
fold change of gene expression (mRNA)
time (s)
0
1
2
3
4
5
0
1000
2000
3000
4000
5000
6000
7000
8000

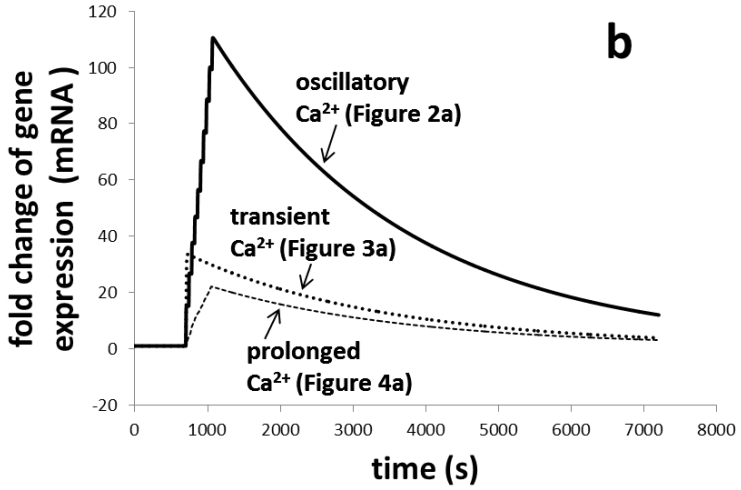
b
oscillatory
Ca2+ (Figure 2a)
transient
Ca2+ (Figure 3a)
prolonged
Ca2+ (Figure 4a)
fold change of gene expression (mRNA)
time (s)
-20
0
20
40
60
80
100
120
0
1000
2000
3000
4000
5000
6000
7000
8000

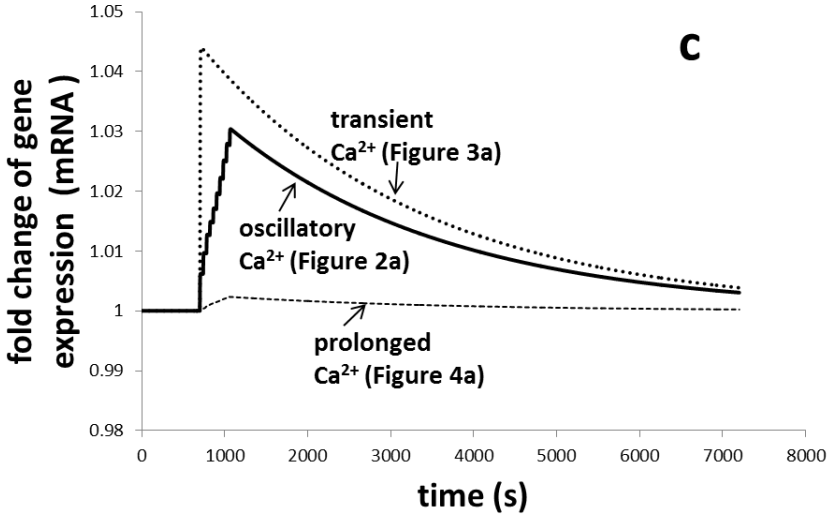
c
transient
Ca2+ (Figure 3a)
oscillatory
Ca2+ (Figure 2a)
prolonged
Ca2+ (Figure 4a)
fold change of gene expression (mRNA)
time (s)
0.98
0.99
1
1.01
1.02
1.03
1.04
1.05
0
1000
2000
3000
4000
5000
6000
7000
8000

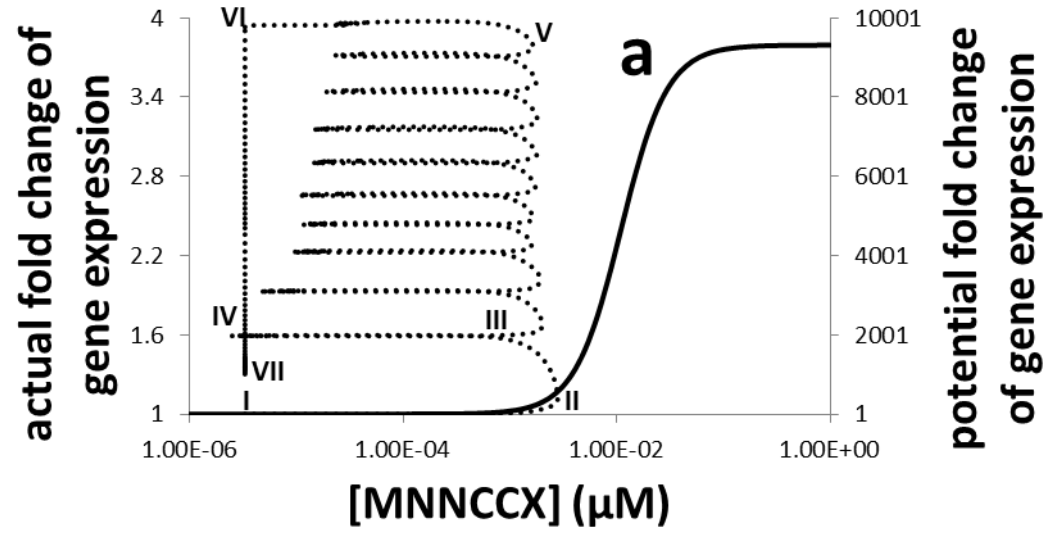
a
actual fold change of gene expression
potential fold change of gene expression
[MNNCCX] (µM)
4
3.4
2.8
2.2
1.6
1
10001
8001
6001
4001
2001
1
1.00E-06
1.00E-04
1.00E-02
1.00E+00
I
II
III
IV
V
VI
VII

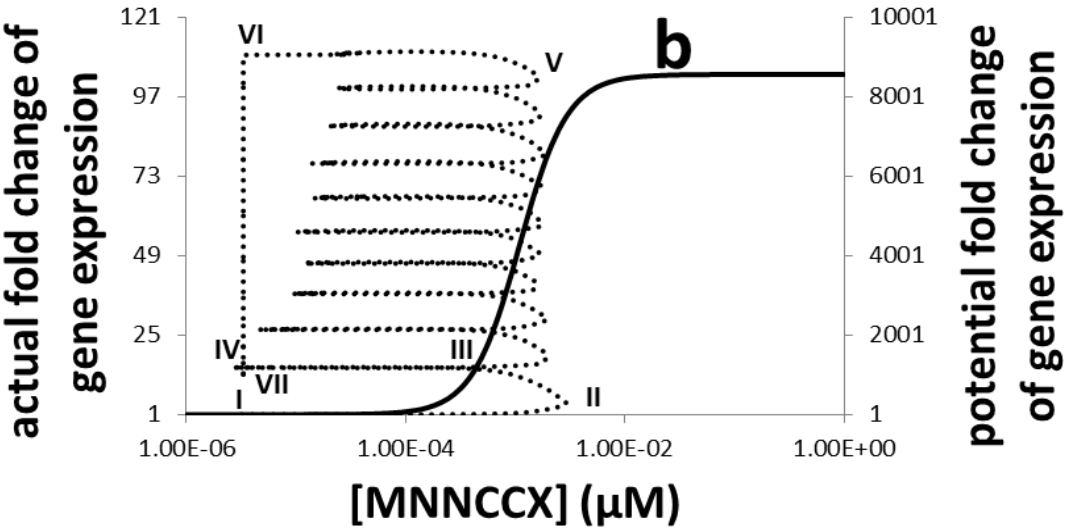
b
actual fold change of gene expression
potential fold change of gene expression
[MNNCCX] (µM)
121
97
73
49
25
1
10001
8001
6001
4001
2001
1
1.00E-06
1.00E-04
1.00E-02
1.00E+00
I
II
III
IV
V
VI
VII

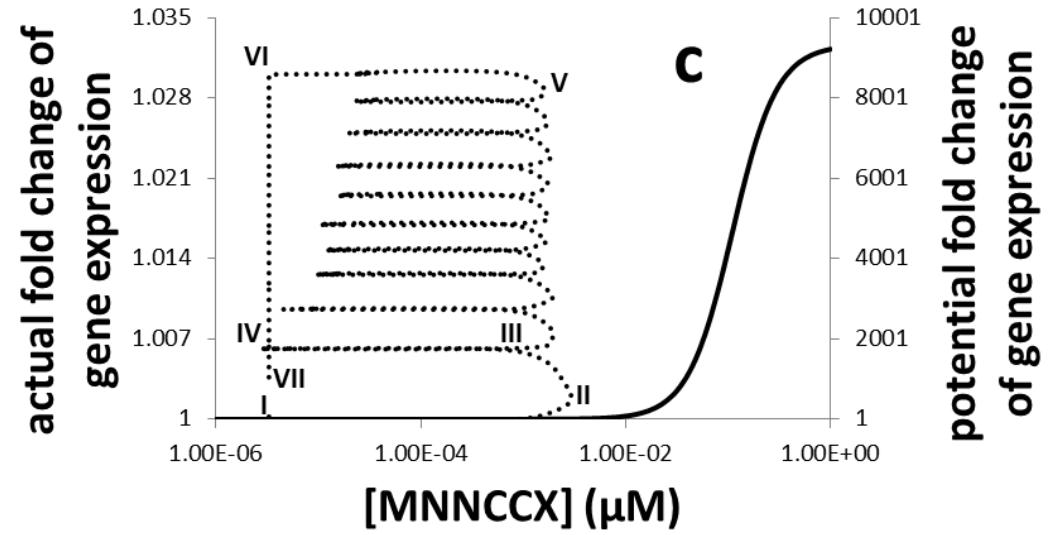
c
actual fold change of gene expression
potential fold change of gene expression
[MNNCCX] (µM)
1.035
1.028
1.021
1.014
1.007
1
10001
8001
6001
4001
2001
1
1.00E-06
1.00E-04
1.00E-02
1.00E+00
I
II
III
IV
V
VI
VII

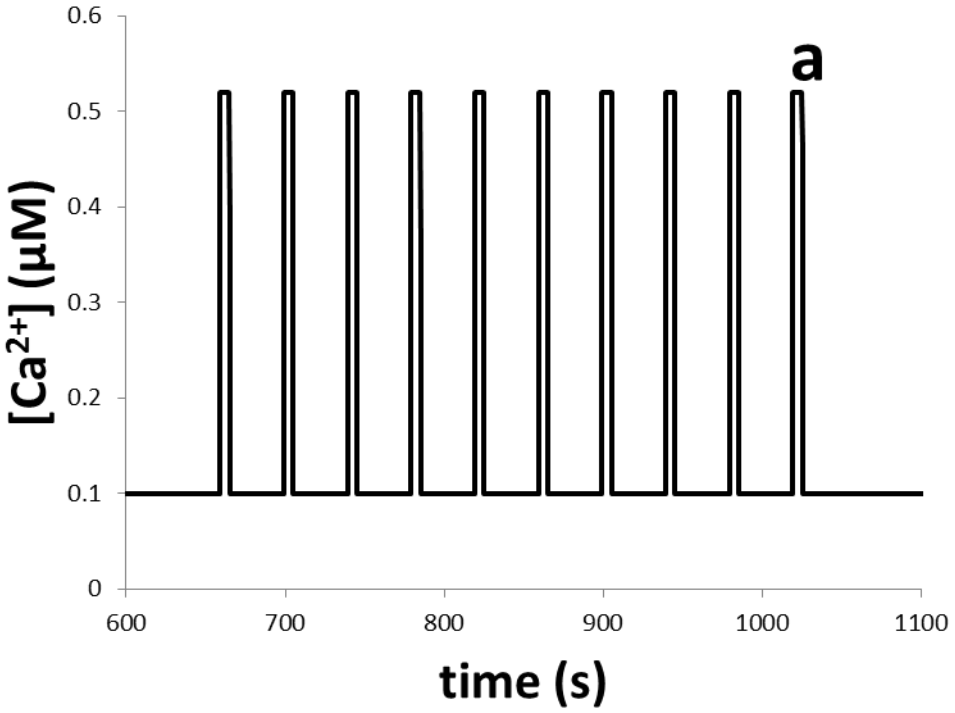
a
[Ca2+] (µM)
0.6
0.5
0.4
0.3
0.2
0.1
0
600
700
800
900
1000
1100
time (s)

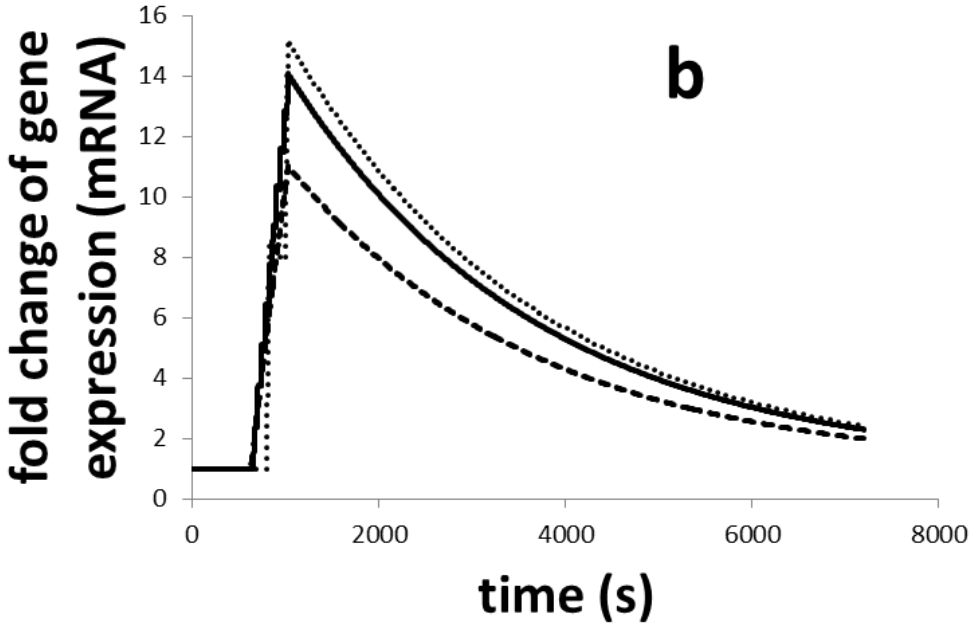
b
fold change of gene expression (mRNA)
16
14
12
10
8
6
4
2
0
0
2000
4000
6000
8000
time (s)